**Supplementary Materials:**

**Materials and Methods:**

**Mice and *in vivo* procedures.** Aged male C57BL/6 mice (22-24 months) were obtained from the National Institutes of Aging (NIA) and young (2-3 months) C57BL/6 (CD45.1$^-$ CD45.2$^+$), B6.SJL (CD45.1$^+$CD45.2$^-$) and *mdx* (C57BL/10ScSn-Dmdmdx/J) male mice were purchased from Jackson Laboratories, Bar Harbor, ME, USA. GFP transgenic mice (C57BL/Ka-β-actin-EGFP (*3-5*)) were bred at the Joslin Diabetes Center and Harvard University. All mice were housed and treated under protocols approved by Institutional Animal Care and Use Committees.

For parabiosis experiments, surgeries were performed as described previously (*11, 13*). Blood chimerism was confirmed in a subset of young isochronic and heterochronic parabiotic pairs by flow cytometry measuring the frequency of donor-derived blood cells from one partner (CD45.1$^+$) in the spleen of the other partner (CD45.2$^+$) after 4 weeks of joining. Partner-derived cells typically represented 40-50% of splenocytes, indicative of establishment of parabiotic cross-circulation (Fig. S5). This method could not be used to verify chimerism in old isochronic pairs, because old CD45.1$^+$ mice are not available for purchase from NIA; however, cross-circulation in aged-isochronic mice has been well established in other studies (*13, 24*). Parabiotic mice were sacrificed after 4 weeks of joining, and muscles were harvested for analysis.

For treatment with rGDF11, mice were randomized into two groups: 1 group was treated with rGDF11 by daily IP injection at 0.1mg/kg of mouse body weight, and the other group was injected with vehicle (PBS containing 0.1% BSA and 4mM HCl). Individual lots of rGDF11 were quality controlled by spectrophotometer, gel electrophoresis and

K562 erythroid differentiation bioactivity assay according to the supplier's recommendations, before use in *in vivo* assays. After 30 days of treatment, unless otherwise specified, mice were sacrificed and muscles harvested for analysis.
For *in vivo* BrdU labeling of proliferating cells, mice were fed BrdU (0.5mg/ml) in drinking water containing 5% sucrose for 4-6 weeks before they were sacrificed and tissues were harvested for analysis.

**Muscle stem cell (satellite cell) isolation and flow cytometry.** Satellite cells were isolated in these studies from intact limb muscles (extensor digitorum longus, gastrocnemius, quadriceps, soleus, tibialis anterior, and triceps brachii) as described previously (*3-5*). After isolation, all myofiber-associated cells were incubated in Hank's Buffered Salt Solution (Gibco) containing 2% donor bovine calf serum on ice for 20 min with the following antibodies: 30-F11 (1:200, anti-mouse CD45, phycoerythrin (PE) or allophycocyanin (APC) conjugate (Biolegend, San Diego, CA)); M1/70 (1:200, anti-mouse CD11b, PE or APC conjugate, (Biolegend, San Diego, CA)); 1:200 anti- mouse Ter119, PE or APC conjugate (Biolegend, San Diego, CA); D7 (1:200, anti-Sca-1, Ly-6A/E, APC conjugate (Biolegend, San Diego, CA)), β1-integrin (1:200, anti-mouse CD29, purified, (BD Pharmingen, San Jose, CA; or 1:100, anti-mouse/rat CD29, PE conjugate (Biolegend, San Diego, CA); CXCR4 (1:100, biotinylated anti-mouse CD184 (BD Pharmingen)), Streptavidin (1:100, Cy7-PE conjugate (eBioscience)), anti-armenian hamster IgG, fluorescein isothiocyanate (FITC) conjugate (1:100, eBioscience). Muscle satellite cells, identified as $CD45^{-}Sca\text{-}1^{-}CD11b^{-}Ter119^{-}CXCR4^{+}$ $\beta1\text{-}Integrin^{+}$ (*3, 4*) were sorted by Fluorescence Activated Cell Sorting (FACS) using Aria II, MoFlo or SORP

Aria (BD Biosciences). Live cells were identified as calcein blue positive (1:1000, Invitrogen, Carlsbad, CA) and propidium iodide negative (PI, 1mg/mL). Satellite cells were double-sorted to maximize purity (*4*). For intracellular staining, myofiber-associated cells were first stained for surface antigen markers and then fixed and permeabilized using cytofix/cytoperm buffer (APC BrdU Flow Kit, BD Pharmingen$^{TM}$) according to the manufacturers' instructions. Cells were subsequently stained with APC-anti-BrdU (APC BrdU Flow Kit, BD Pharmingen$^{TM}$), or anti-activated (cleaved) caspase-3 (Asp175) Alexa-488conjugate (1:50, Cell signaling), or anti-phospho-53BP1 (S25) (1:50, Bethyl laboratories). If secondary antibody staining was required, cells were first blocked with goat serum (1/100) and anti-CD16/32 NA/LE (2.4G2, BD) and then stained with goat-anti-rabbit-Alexa488 (1:100, Invitrogen). For studies of activated caspase-3 or phospho-53BP1 expression, a subset of myofiber-associated cells was treated with 950μM $H_2O_2$ at 37°C for 2 hours to generate a positive control for staining, and a distinct subset was stained with secondary antibody alone to serve as negative control, as indicated. Flow cytometry data were collected using DIVA (Becton Dickinson (BD), Franklin Lakes, NJ) and analyzed offline using Flowjo software (Tree Star, Inc., version 8.6.1, Ashland, OR).

**Single Cell Gel Electrophoresis Assay.** For single cell gel electrophoresis assay (also called Comet Assay), ~3000 satellite cells were double-sorted into Eppendorf tubes containing 350μl of Hank's Buffered Salt Solution (Gibco) with 2% donor bovine calf serum. The myogenic purity of this population is >98%, as assessed by Pax7-immunostaining (Fig. S1 and (*4, 5*)). Single cell gel electrophoresis assay was performed according to manufacturer's specifications (Cell Biolabs, Inc. San Diego, CA). Briefly, cells were centrifuged at 700rcf for 3 min. at room temperature and the cell pellet was

resuspended with molten low-melting point agarose pre-incubated at 37°C for at least 20 min. The cell-agarose suspension was then applied gently onto slides and allowed to form a thin layer. The agarose layer was further solidified on ice before submersion in lysis buffer (Cell Biolabs, Inc.). Cell lysis was carried out for 12 hours at 4°C and DNA was then electrophoresed in neutral or alkaline electrophoresis buffer. Extreme care was taken to minimize exposure to light during sorting and subsequent processing and handling of cells until electrophoresis. Finally, electrophoresed and VistaDye stained DNA was visualized using a Zeiss Imager M1 Fluorescence microscope (Carl Zeiss, Thornwood, NY), and 100-250 nuclei per animal were visually scored according to published protocols (*25*). This scoring approach has been documented to be equally effective for detecting differences as other methods (e.g. calculation of tail moment) (*25*).

**Immunofluorescence.** For immunostaining of cells, ~5000 satellite cells were sorted directly onto slides and into a small droplet of PBS. Cells were allowed to settle on ice for 30 minutes before fixation with 4% PFA for 20 minutes at room temperature. Immunostaining of single myofibers was performed on dissected hindlimb muscles (extensor digitorum longus, gastrocnemius, quadriceps, soleus, tibialis anterior, and triceps brachii) from young (2 mo.) and old (24 mo.) mice. Dissected muscles were digested with 0.2% collagenase type II, minced, and fixed in 4% paraformaldehyde in PBS. Fixed cells or single myofibers were washed with PBS, permeabilized and blocked using 2% BSA/0.5% Goat Serum/ 0.5% Triton X in PBS for 60 min. at room temperature. For immunostaining with primary antibodies raised in mouse, the M.O.M immunodetection kit (Vector Laboratories, Burlingame, CA) was used. Primary antibodies (mouse monoclonal anti-Pax7 (1:100 DSHB, University of Iowa), rabbit

polyclonal anti-pH2AX (1:500, Abcam), anti-cleaved caspase-3 (Asp175) AlexaFluor 488 conjugate (1:50, Cell signaling), or rabbit polyclonal anti-53BP1 (1: 50, Novus Biological) were incubated with samples for 12-16 hours at 4°C or 1 hr at RT, and secondary antibodies (1:200, AlexaFluor 555, AlexaFluor 488 or AlexaFluor 594 Invitrogen) for 60 min. at room temperature (with 3-4 washes in PBS following each incubation). For 53BP1 immunostaining, serum block (10% goat serum) and detergent (0.1% Tween20) were included during both primary and secondary antibody incubations. Single myofibers, were additionally washed once with PBS containing 0.01% Tween20, after secondary antibody staining. All samples were mounted on slides in Vectashield mounting medium containing DAPI (Vector Laboratory). 50-100 fluorescence images of sorted cells per sample were obtained using a Zeiss Imager M1 Fluorescence microscope (Carl Zeiss, Thornwood, NY) and quantified using ImageJ. 50-100 confocal images of sorted cells per sample were obtained using an Inverted LSM 510 Meta or Inverted LSM 700 Meta (Carl Zeiss, Thornwood, NY) and quantified using AIM software and ImageJ.

**Neuromuscular junction immunofluorescence.** Extensor digitorum longus (EDL) muscles were fixed for 1 hour at room temperature (4% paraformaldehyde in PBS). Unless otherwise indicated, all incubations were performed at room temperature. EDL muscles were teased into bundles of muscle fibers. Muscles were washed twice for 15 min in PBS, incubated 15 min with 100 mM glycine in PBS, and rinsed in PBS. After removal of the overlying connective tissue, muscles were permeabilized and blocked for 1 hr in PBS containing 2% bovine serum albumin, 4% normal goat serum, and 0.5% Triton X-100. To quantify the number and density of acetylcholine receptors (AChRs),

muscles were stained with AlexaFluor 594 α-Bungarotoxin (BTX), first for 1 hr at room temperature and then overnight at 4°C. After three 30 min washes in PBS, muscles were rinsed in PBS, fixed 30 min with 1% formaldehyde in PBS, washed three times for 10 min in PBS, and flat-mounted in Vectashield with DAPI (Vector Laboratories, Burlingame, CA). Images were acquired using a Zeiss M1 or LSM 510 confocal microscope.

**Myogenesis assays.** Muscle satellite cells from young or aged mice were clone-sorted (single cell/well) or bulk-sorted (200 cells/well) into 96-well plates containing growth medium (F10, 20% horse serum, 1% Glutamax and 1% pen/strep) using the automated cell deposition unit (ACDU) of the Aria II (BD Biosciences). Prior to sorting, 96-well plates were coated with collagen/laminin by incubating the wells with PBS containing collagen (1mg/ml, Sigma) and laminin (10mg/ml, Invitrogen) for at least an hour at 37°C. Satellite cells were cultured in growth media comprised of F10, 1% glutamax, 1% Pen-strep and 20% horse serum or knock-out serum replacement (KOSR, Invitrogen), where indicated, with fresh bFGF added daily at 5ng/ml final concentration. Purified recombinant GDF11 (rGDF11, catalog # 120-11, PeproTech), resuspended in PBS containing 0.1% BSA and 4mM HCl, was added daily at the concentrations indicated. Individual lots of rGDF11 were quality controlled by spectrophotometer, gel electrophoresis and K562 erythroid differentiation bioactivity assay according to the manufacturere's recommendations, before use in *in vitro* assays. Wells containing myogenic colonies were either counted by brightfield microscopy or fixed with 4% PFA and the number of cells per well was counted on a Celigo automated microscope as

Hoechst-stained nuclei at the indicated time points. For differentiation assays, satellite cells were sorted into 24-well plates at 5000 cells per well. Cells were cultured in growth media (described above) supplemented with bFGF for 5 days. At 5-8 days after plating, media were changed to differentiation media (DMEM, 1% GlutaMax, 1% pen-strep, and 2% FBS) and cultured for an additional 3-7 days. For differentiation analyses, myotubes were stained with anti-fast myosin (Sigma), DAPI, and AlexaFluor 488 conjugated Phalloidin (Life Technologies). For mitochondrial staining on myotubes, satellite cells were proliferated and differentiated into myotubes on 24-well plate compatible for microscope imaging (ibidi μ-plate). After 5 days in differentiation media, myotubes were washed in PBS and incubated in 250 nM Mitotracker Orange for 1 hr at 37°C. Cells were washed twice and fixed in 2% paraformaldehyde for 10 min. at room temperature. Myotubes were counterstained with DAPI and Phalloidin (Life Technologies). Images were acquired using a Zeiss Observer D1 inverted microscope.

**Muscle Injury and muscle sectioning.** Tibialis anterior (TA) muscles of anesthetized mice were cryoinjured or injured with cardiotoxin (at 0.3mg/ml) one week before harvest. Harvested muscles were fixed in 4% PFA and embedded in paraffin for sectioning. H&E staining was performed on 8-10 μm paraffin-embedded sections for quantification of centrally nucleated regenerating myofibers of injured and contralateral, uninjured TA muscles. For each sample, cross sectional area of 120-150 regenerating myofibers were blindly measured from 4 slides with 3 consecutive sections on each slide.

**Satellite cell transplantation.** Anesthetized *mdx* mice were injected with 25µl (0.03 mg/ml) of Naja mossambica mossambica cardiotoxin (Sigma) into TA muscles 1 day prior to cell transplantation. The next day, double-sorted satellite cells isolated from 6-8 weeks old GFP transgenic mice (C57BL/Ka-β-actin-EGFP (*3-5*)) and irradiated with gamma-irradiation at indicated dosages (0, 50 or 100 rad) were resuspended in 5–10µl PBS and injected directly into these pre-injured muscles. Injected TA muscles were harvested 4 weeks after transplant, snap-frozen in liquid nitrogen cooled methylbutane, and serially sectioned throughout the TA muscle from tendon to belly using Microm HM550 cryostat (Thermo Scientific). For transplantation experiments in aged mice, male mice (22 months old) were randomized into control (PBS, n=4) or rGDF11 (n=4) groups and treated as described above. After 4 weeks of vehicle or rGDF11 treatment, TA muscles were injured with cardiotoxin and $GFP^+$ satellite cells (30,000 per leg) were transplanted the following day. Injected TA muscles were harvested 2 weeks after transplant, frozen muscle sections were processed for immunofluorescence as described above. Briefly, sections were fixed in 4% PFA for 1hr and washed three times in PBS for 10 min at RT. Sections were counterstained with Alexa488 conjugated anti-GFP and AlexaFluor 555 conjugated Phalloidin (Life Technologies) and mounted with Vectashield with DAPI (Vector Laboratory). 7-8 slides per muscle and 10-12 sections per slide from each experimental group were prepared and analyzed blindly to determine the maximum number of engrafted ($GFP^+$) fibers and cross-sectional area of engrafted fibers using Axiovision software (Zeiss).

**Physical Endurance test**. For endurance exercise testing, vehicle- or rGDF11-treated aged (24 mo. of age) C57Bl/6 male mice were exercised using an adjustable variable

speed belt treadmill (AccuPacer, AccuScan Instruments, Inc). Animals were first acclimated to the treadmill by walking at 5 meters per minute (mpm) with inclination set at 0° for 5 minutes. The speed and inclination of the treadmill were gradually increased in a step-wise manner to a maximum of 20 mpm and 15° respectively. Animals were exercised on the treadmill for a maximum of 90 minutes or until they were exhausted. Exhaustion was determined by refusal of mice to remain on the treadmill for at least 20 seconds.

**Measurement of biochemical metabolites after treadmill exercise**. Immediately following a 20 min bout of exercise, the tails of exercised mice were nicked with a scalpel and the tail vein was massaged to obtain an appropriate volume of blood (approximately 3 μl) for both glucose and lactate measurements. Blood glucose was measured using an OneTouch® Ultra Blood Glucose Meter (Lifescan). Blood lactate was measured using the Lactate Plus Meter (Nova Biomedical). Measurements of glucose and lactate levels during exercise were performed at the indicated time point (i.e., at 0, 20, 40, 60 minutes of running, and at exhaustion).

**Grip-strength test.** For measurement of *in vivo* muscle force and neuromuscular function, vehicle- or rGDF11-treated (for 4 weeks) aged (25 mo. of age) C57Bl/6 male mice were allowed to grasp onto the horizontal metal grid of the grip strength meter (Columbus Instruments, Columbus, Ohio) by using only the forelimbs and pulled backwards 3 times. The force applied to the grid each time before the animal lost its grips was recorded in Newton. The maximum force in Newton was also normalized to the body weight of each animal and represented in the data.

**ELISA and Western.** For ELISA, crushed muscle (tibialis anterior) extracts (10mg/ml) or plasma harvested from young (2-3 mo.) and aged male C57BL/6 mice (24 mo.) were diluted as indicated and used on TGF-β1 Immunoassay Quantikine® ELISA Catalog # MB100B and Myostatin Immunoassay Quantikine® ELISA Catalog # DGDF80 (R&D systems, Minneapolis, MN) as per manufacturer's instructions. For Westerns, 100 μg of plasma or whole muscle (quadriceps or gastrocnemius) extracts were loaded onto appropriate (4-20%) gradient Criterion Tris-HCl polyacrylamide gels (Biorad Labs) and immunoblotted for proteins as indicated using the following antibodies: anti-GDF11 (Abcam rabbit mAb 1:1000), anti-GDF11 (mouse mAb 1:500, obtained from Richard Lee), anti-PGC-1α (1:1000, Santa Cruz), and anti LC3B (1:1000, Novus). Densitometric quantification of Western data were normalized to GAPDH (1:2000, Santa Cruz) or Actin (1:1000, Sigma) serving as loading controls.

**Mitochondrial Function Assay.** The rate of oxygen consumption (OCR) was measured using Seahorse Bioscience extracellular flux analyzer (XF24). FACS isolated satellite cells were seeded into 24-well plates at a density of 5000/well and differentiated into myotubes as described above. Basal and maximal oxygen consumption rates (OCR) were calculated by comparing values with or without the mitochondrial uncoupler, FCCP (5μM). The final OCR values (pmol/min) were normalized to total protein concentration per well.

**Transmission Electron Microscopy (TEM).** Tissue processing for TEM was done at the University of Texas Pathology Core. Briefly, muscle blocks (1 $mm^3$ in size) from tibialis

anterior muscle were incubated in fixative (2% paraformaldehyde, 2.5% gluteraldehyde, and 0.1 M sodium cacodylate) for 2 hours in room temperature then post-fixed with 1% osmium tetroxide followed by 1% uranyl acetate. The blocks were then dehydrated through a graded series of ethanol washes and embedded in resin. Blocks were cut in ultrathin (80 nm) sections on Reichert Ultracut UCT, stained with uranyl acetate followed by lead citrate and imaged on a JEOL 1230 EX transmission electron microscope at 80kV.

**RNA transcriptome analysis**. RNA transcriptome analysis was performed using Affymetrix GeneChip Mouse Genome 430 2.0 arrays. Raw microarray data have been deposited in the Gene Expression Omnibus database. www.ncbi.nlm.nih.gov/geo (GSE50821). A subset of differentially expressed myogenic transcripts was chosen to generate a heatmap from the original dataset normalized by gcRMA algorithm and SAM cutoff (<10% q-values) using R statistical software.

Figure S1

A

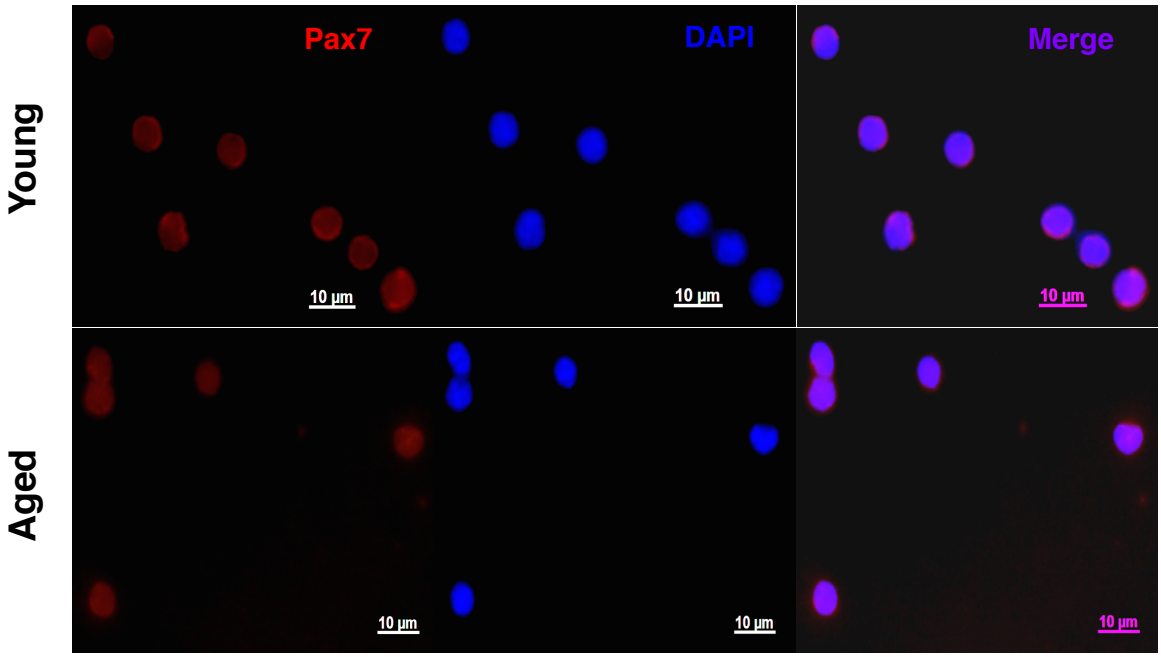
Young
Aged
Pax7
DAPI
Merge
10 μm

B

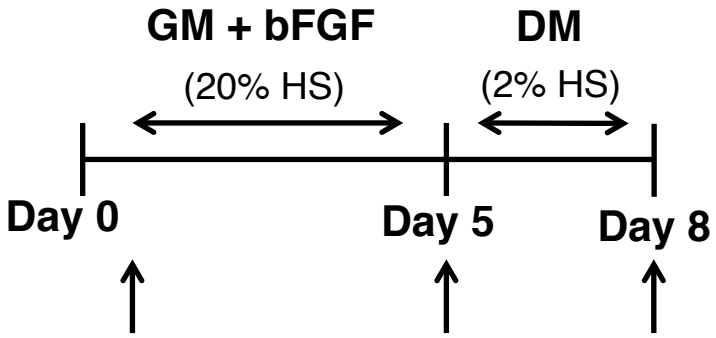
GM + bFGF
(20% HS)
DM
(2% HS)
Day 0
Day 5
Day 8

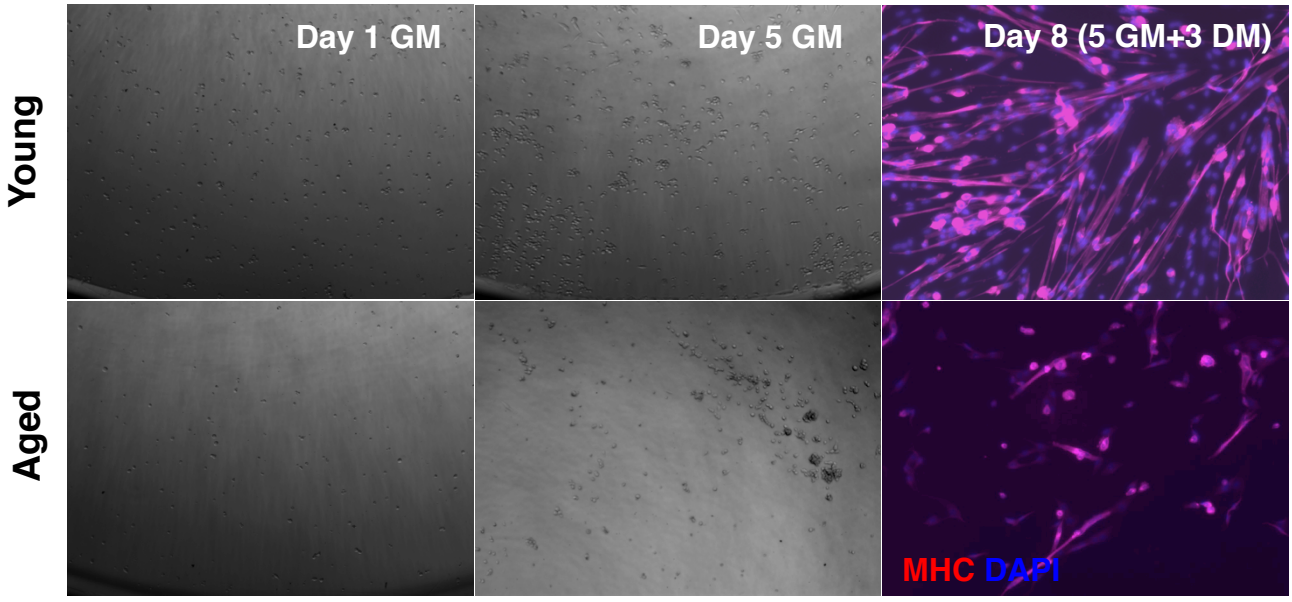
Young
Aged
Day 1 GM
Day 5 GM
Day 8 (5 GM+3 DM)
MHC DAPI

# Figure S2

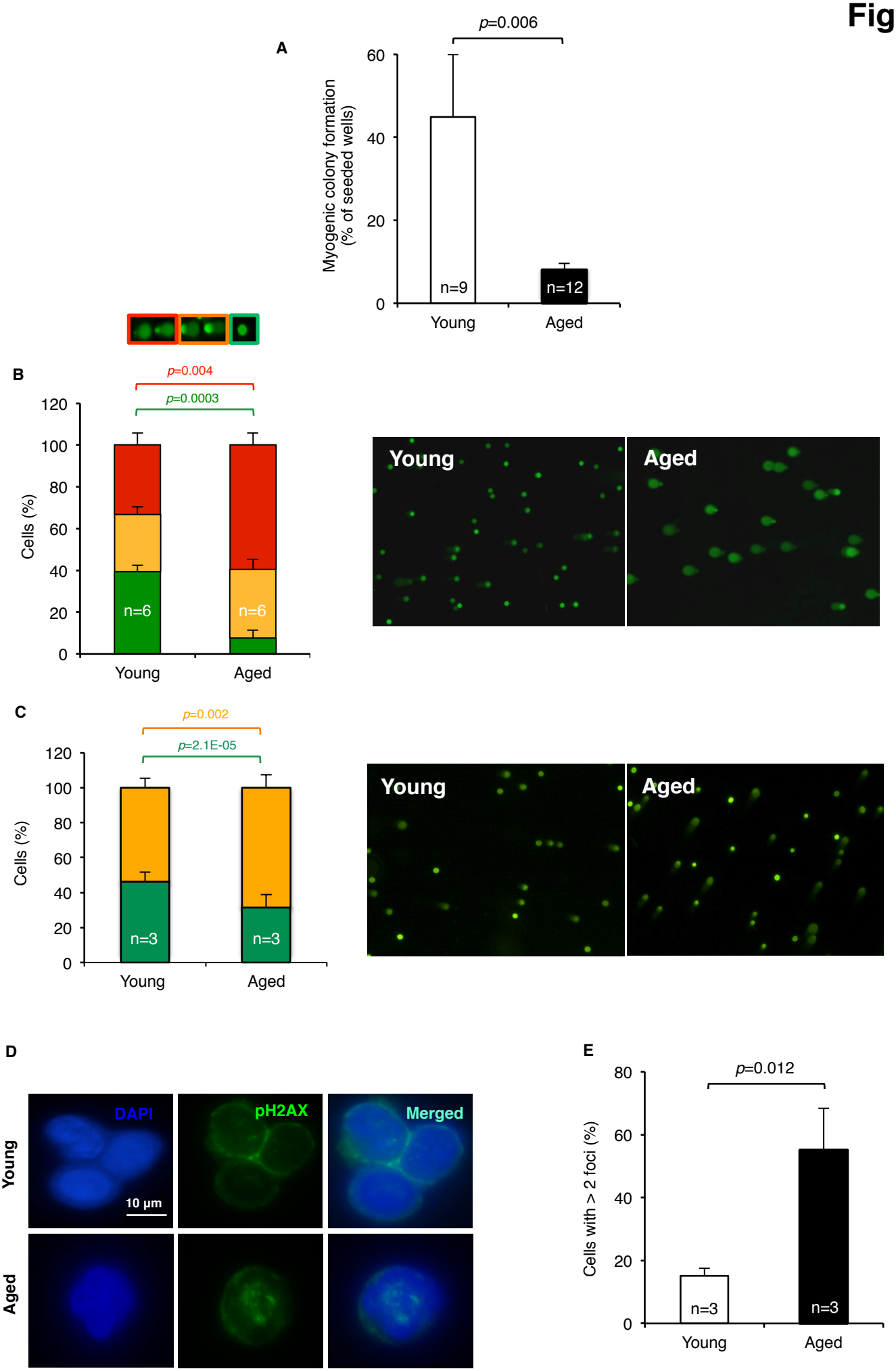
A
p=0.006
Myogenic colony formation (% of seeded wells)
60
40
20
0
n=9
n=12
Young
Aged
B
p=0.004
p=0.0003
Cells (%)
120
100
80
60
40
20
0
n=6
n=6
Young
Aged
Young
Aged
C
p=0.002
p=2.1E-05
Cells (%)
120
100
80
60
40
20
0
n=3
n=3
Young
Aged
Young
Aged
D
DAPI
pH2AX
Merged
Young
Aged
10 µm
E
p=0.012
Cells with > 2 foci (%)
80
60
40
20
0
n=3
n=3
Young
Aged

Figure S3

A

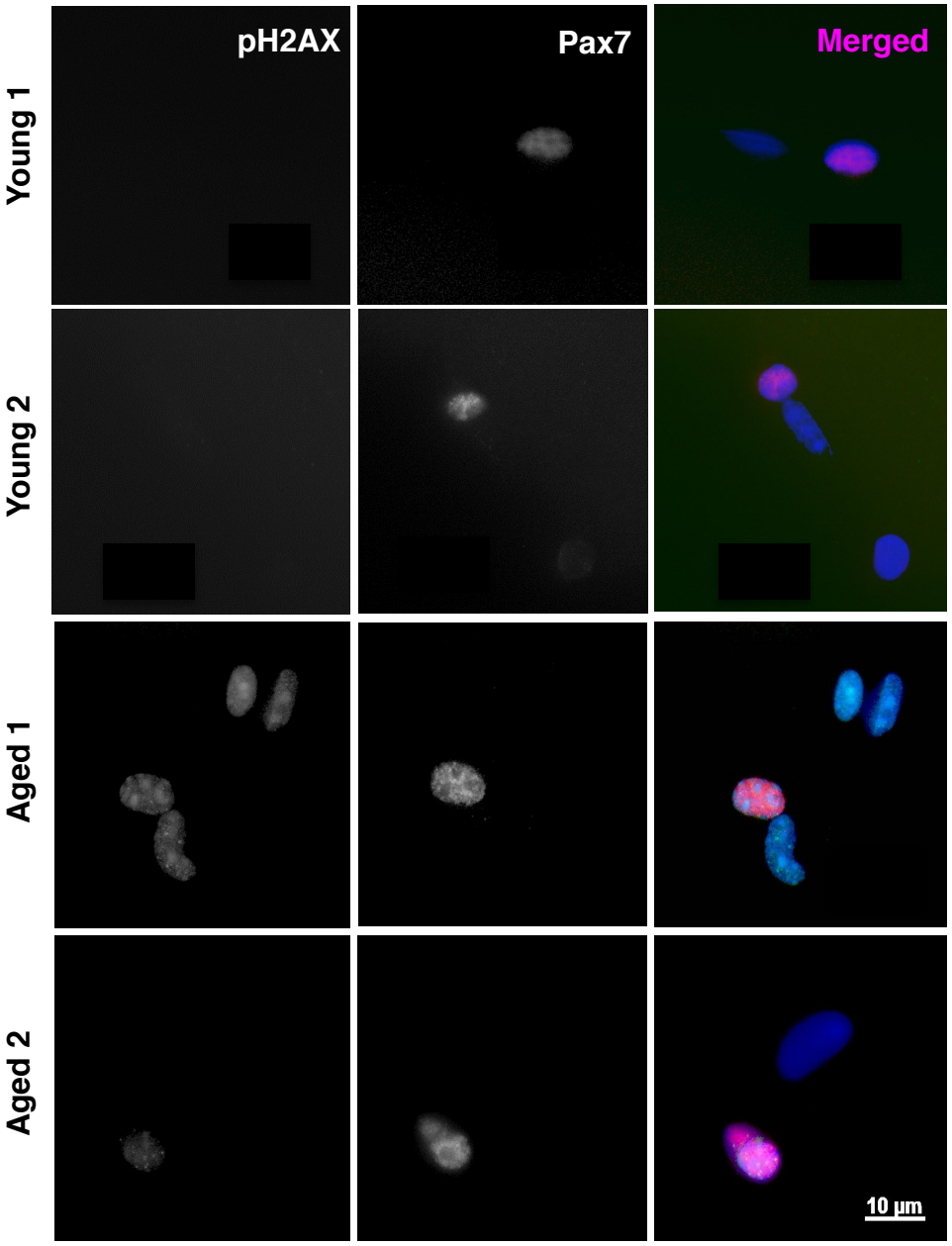
pH2AX
Pax7
Merged
Young 1
Young 2
Aged 1
Aged 2
10 µm

B

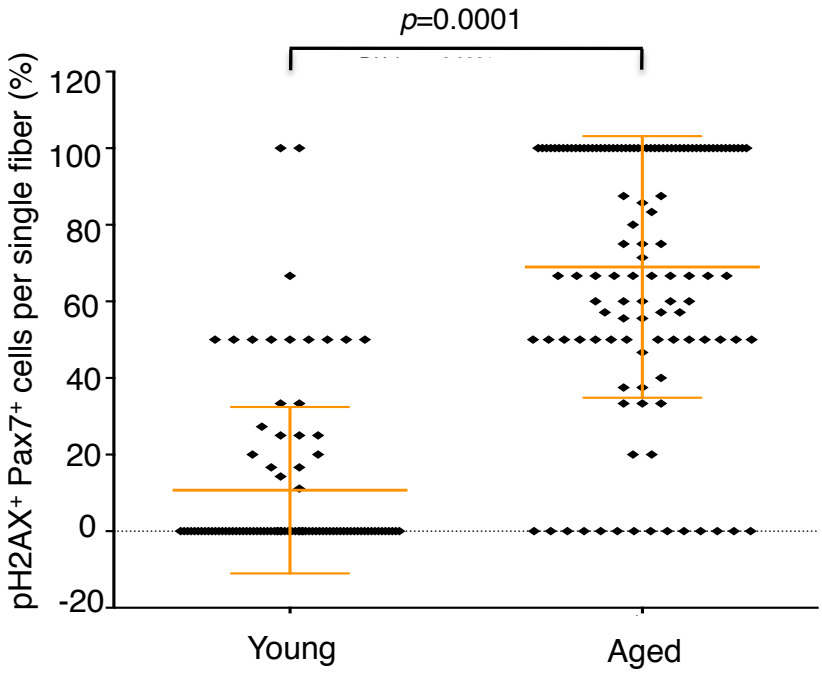
p=0.0001
pH2AX+ Pax7+ cells per single fiber (%)
120
100
80
60
40
20
0
-20
Young
Aged

# Figure S4

**A**

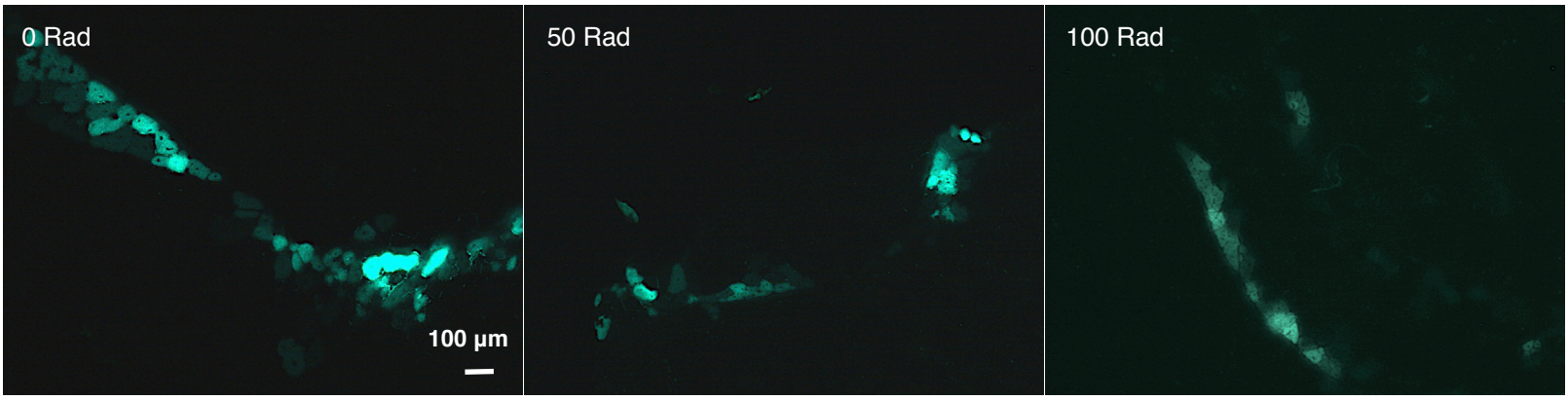


**B**

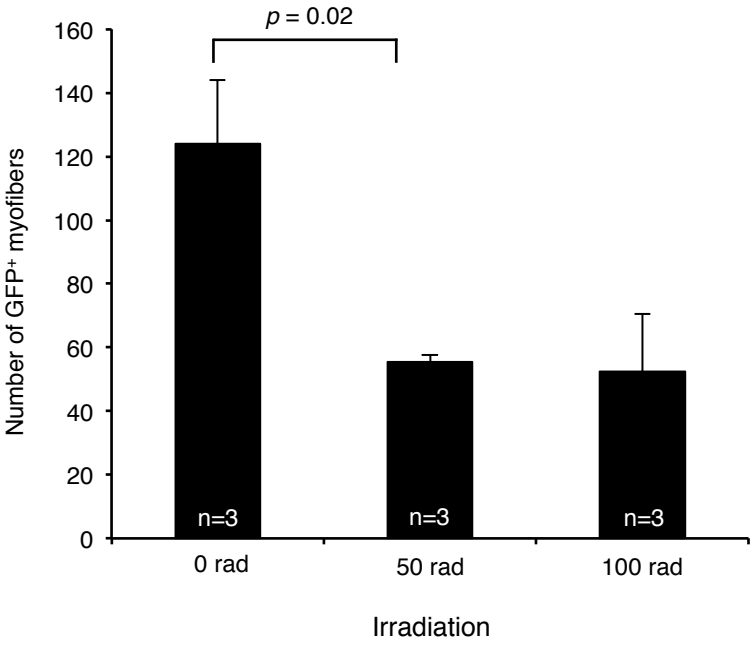


**C**

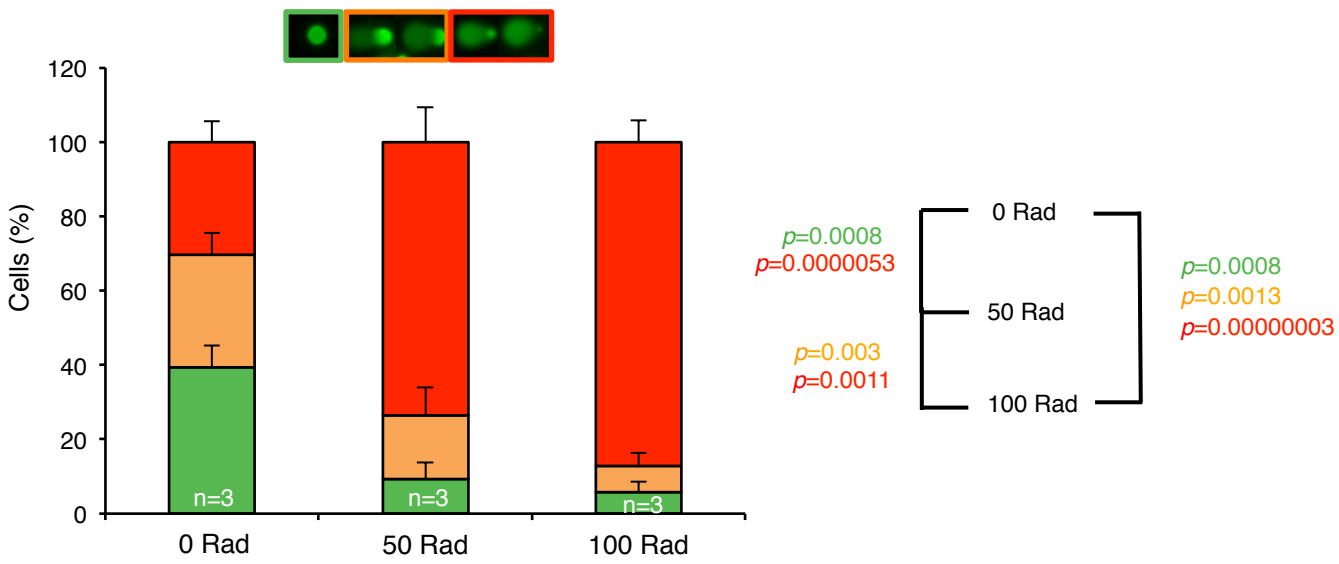

# Figure S5

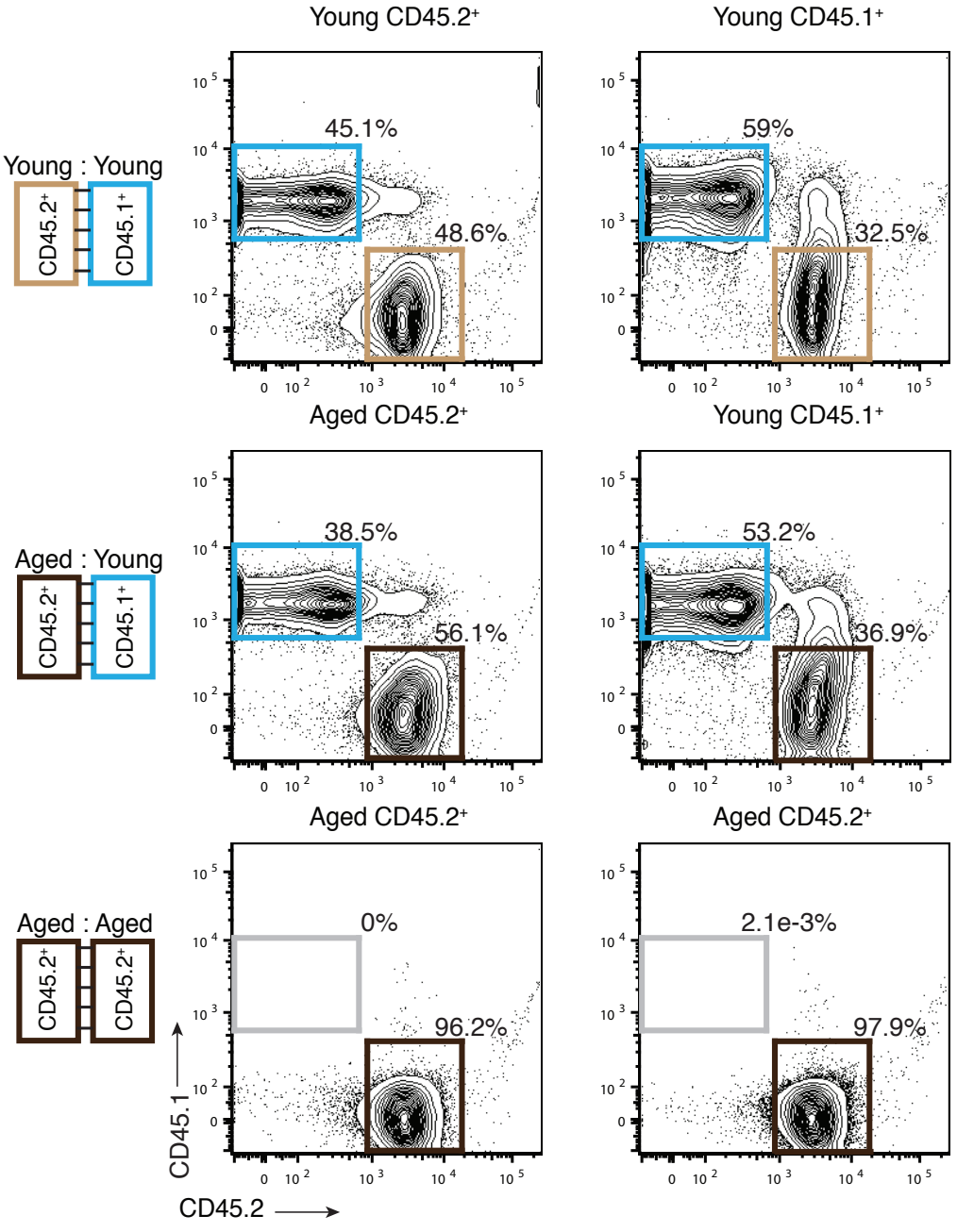
Young CD45.2+
Young CD45.1+
Young : Young
CD45.2+
CD45.1+
45.1%
48.6%
59%
32.5%
Aged CD45.2+
Young CD45.1+
Aged : Young
38.5%
56.1%
53.2%
36.9%
Aged CD45.2+
Aged CD45.2+
Aged : Aged
0%
96.2%
2.1e-3%
97.9%
CD45.1
CD45.2

**Figure S6**

**A**

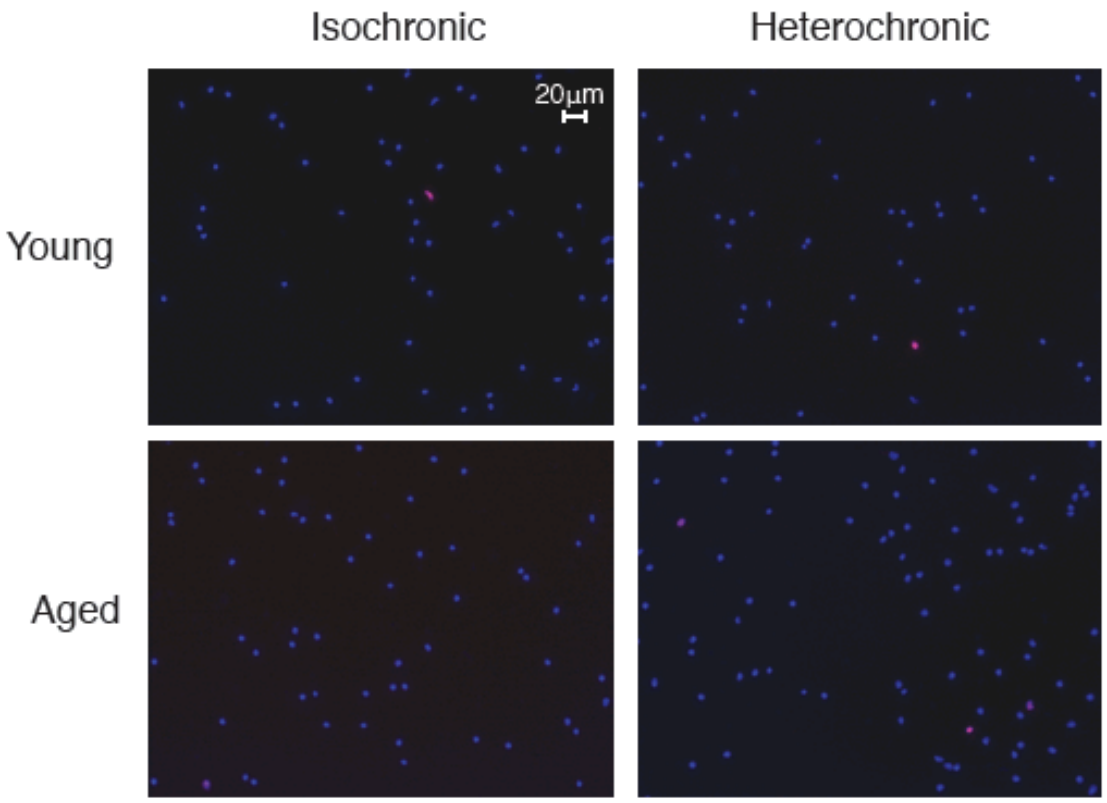
Isochronic
Heterochronic
20μm
Young
Aged

**B**

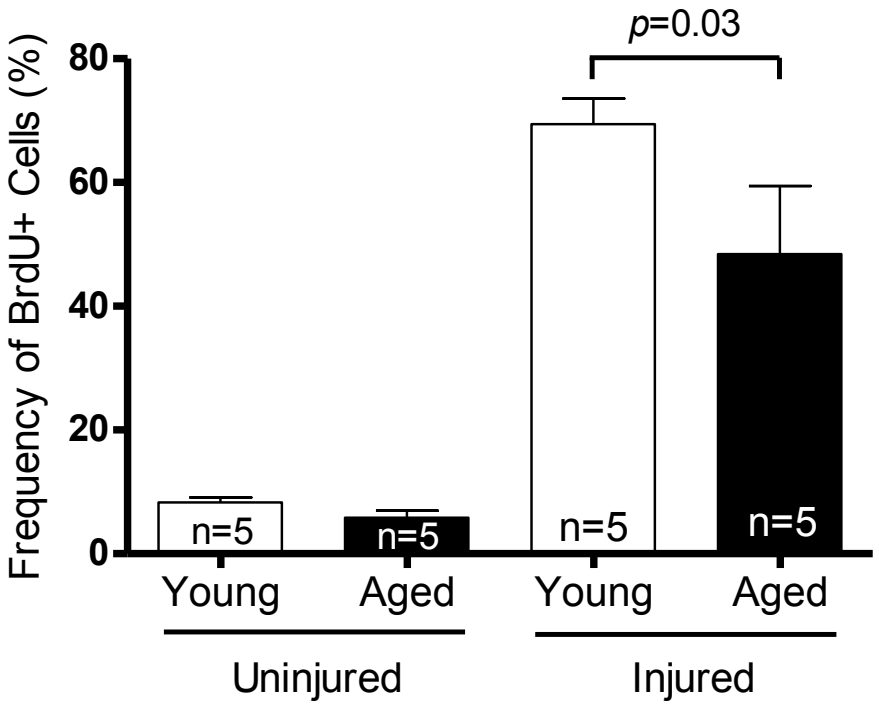
p=0.03
Frequency of BrdU+ Cells (%)
80
60
40
20
0
n=5
n=5
n=5
n=5
Young
Aged
Young
Aged
Uninjured
Injured

# Figure S7

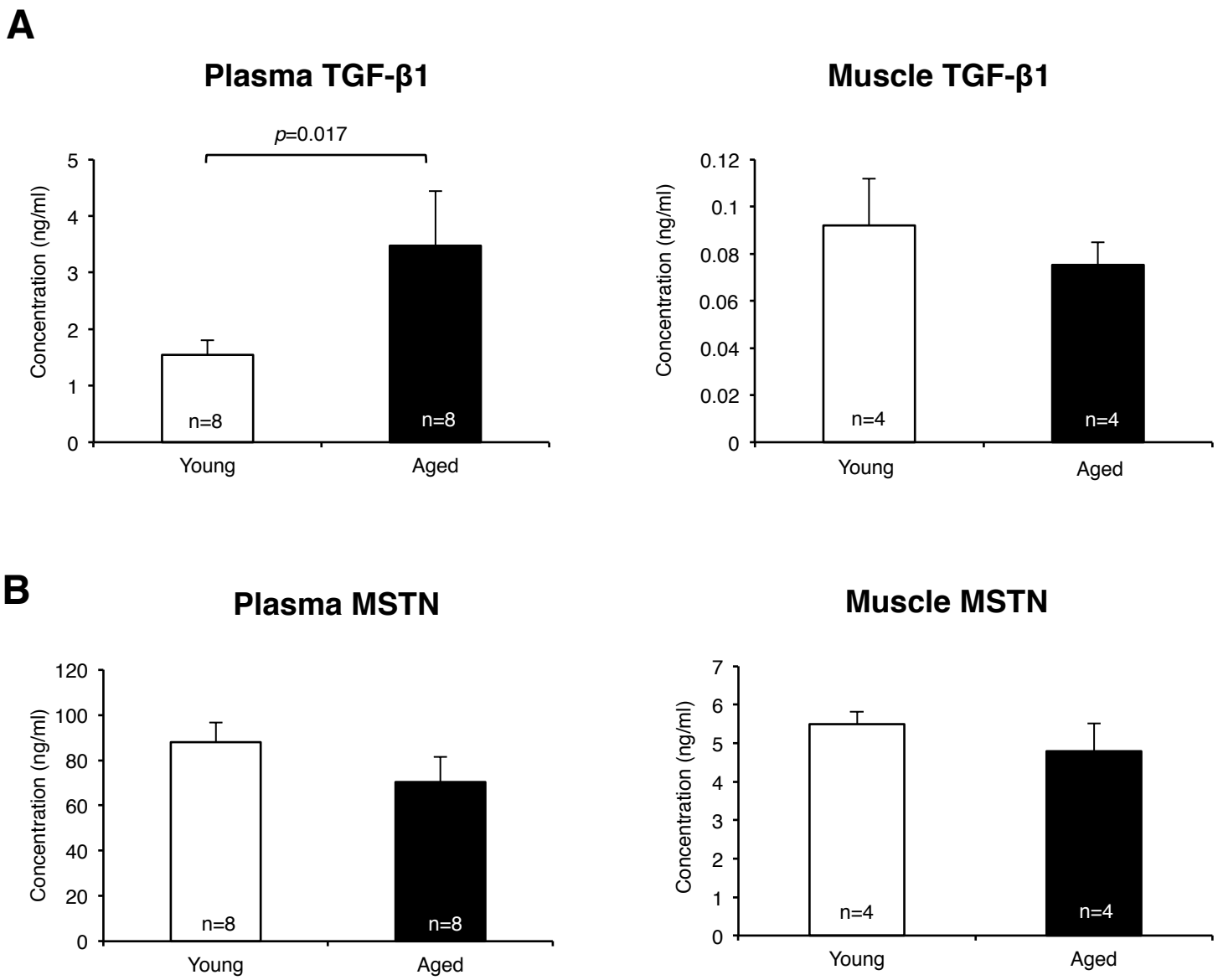
A
Plasma TGF-β1
p=0.017
Concentration (ng/ml)
0
1
2
3
4
5
n=8
n=8
Young
Aged
Muscle TGF-β1
Concentration (ng/ml)
0
0.02
0.04
0.06
0.08
0.1
0.12
n=4
n=4
Young
Aged
B
Plasma MSTN
Concentration (ng/ml)
0
20
40
60
80
100
120
n=8
n=8
Young
Aged
Muscle MSTN
Concentration (ng/ml)
0
1
2
3
4
5
6
7
n=4
n=4
Young
Aged
C
rGDF11
Young + Vehicle
Young + rGDF11
Aged + Vehicle
Aged + rGDF11
Plasma
12.5 kDa
Young + Vehicle
Aged + Vehicle
Aged + rGDF11
Muscle
12.5 kDa

**Figure S8**

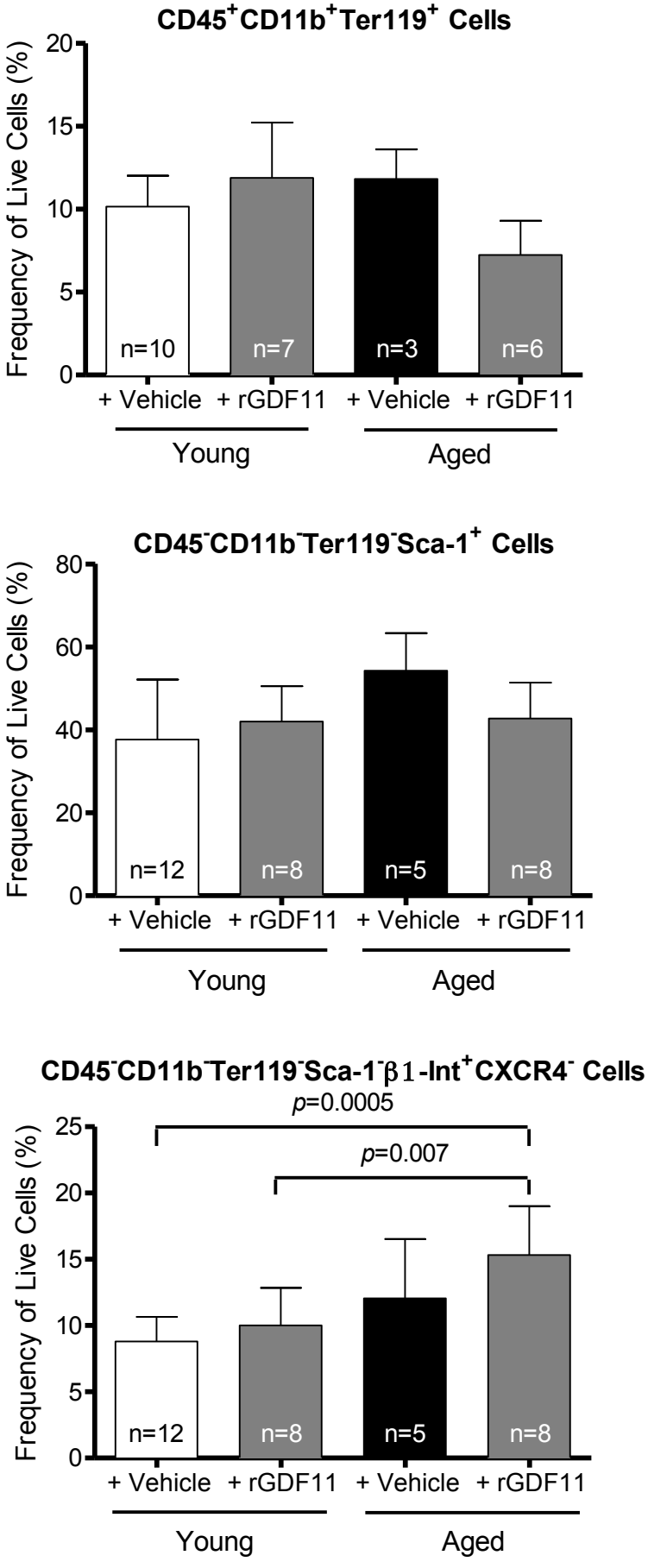
CD45+CD11b+Ter119+ Cells
Frequency of Live Cells (%)
20
15
10
5
0
n=10
n=7
n=3
n=6
+ Vehicle
+ rGDF11
+ Vehicle
+ rGDF11
Young
Aged
CD45-CD11b-Ter119-Sca-1+ Cells
Frequency of Live Cells (%)
80
60
40
20
0
n=12
n=8
n=5
n=8
+ Vehicle
+ rGDF11
+ Vehicle
+ rGDF11
Young
Aged
CD45-CD11b-Ter119-Sca-1-β1-Int+CXCR4- Cells
p=0.0005
p=0.007
Frequency of Live Cells (%)
25
20
15
10
5
0
n=12
n=8
n=5
n=8
+ Vehicle
+ rGDF11
+ Vehicle
+ rGDF11
Young
Aged

# Figure S9

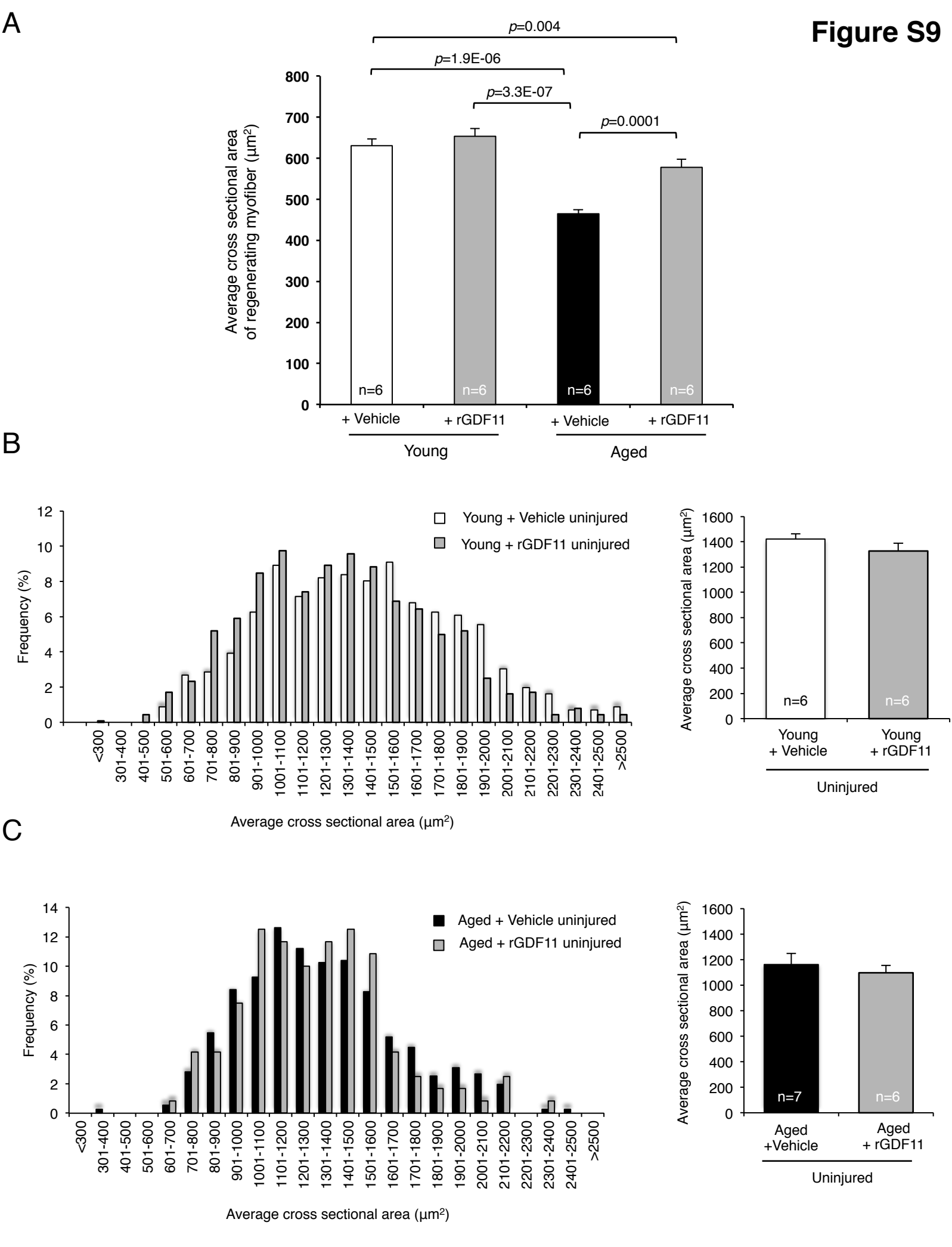
A
p=0.004
p=1.9E-06
p=3.3E-07
p=0.0001
Average cross sectional area of regenerating myofiber (μm²)
800
700
600
500
400
300
200
100
0
n=6
n=6
n=6
n=6
+ Vehicle
+ rGDF11
+ Vehicle
+ rGDF11
Young
Aged
B
Young + Vehicle uninjured
Young + rGDF11 uninjured
Frequency (%)
12
10
8
6
4
2
0
<300
301-400
401-500
501-600
601-700
701-800
801-900
901-1000
1001-1100
1101-1200
1201-1300
1301-1400
1401-1500
1501-1600
1601-1700
1701-1800
1801-1900
1901-2000
2001-2100
2101-2200
2201-2300
2301-2400
2401-2500
>2500
Average cross sectional area (μm²)
Average cross sectional area (μm²)
1600
1400
1200
1000
800
600
400
200
0
n=6
n=6
Young + Vehicle
Young + rGDF11
Uninjured
C
Aged + Vehicle uninjured
Aged + rGDF11 uninjured
Frequency (%)
14
12
10
8
6
4
2
0
<300
301-400
401-500
501-600
601-700
701-800
801-900
901-1000
1001-1100
1101-1200
1201-1300
1301-1400
1401-1500
1501-1600
1601-1700
1701-1800
1801-1900
1901-2000
2001-2100
2101-2200
2201-2300
2301-2400
2401-2500
>2500
Average cross sectional area (μm²)
Average cross sectional area (μm²)
1600
1400
1200
1000
800
600
400
200
0
n=7
n=6
Aged +Vehicle
Aged + rGDF11
Uninjured

# Figure S10

**A**

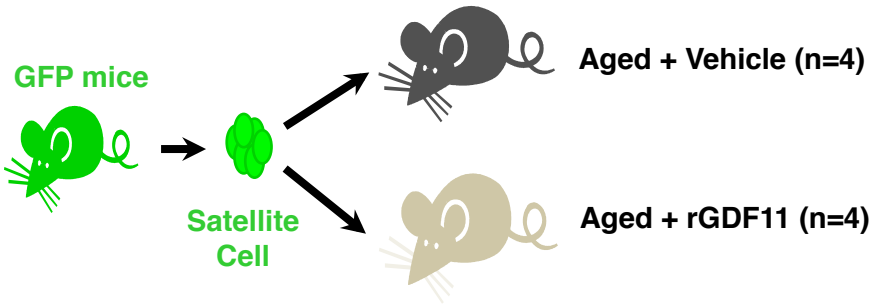


**B**

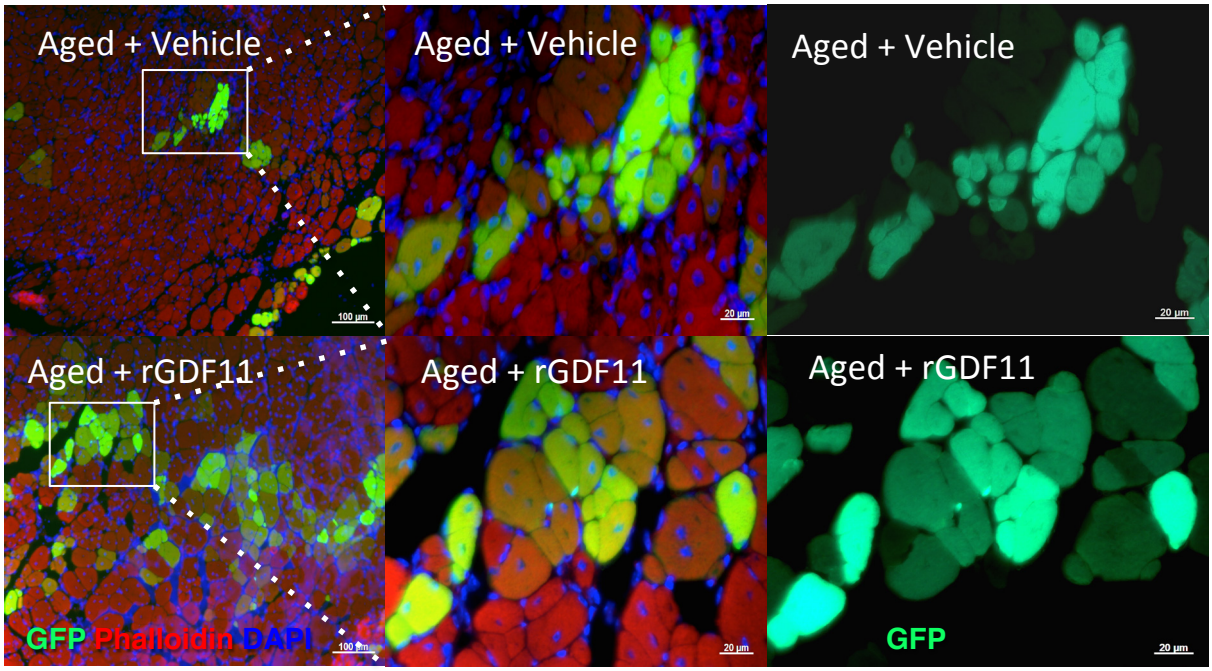


**C**

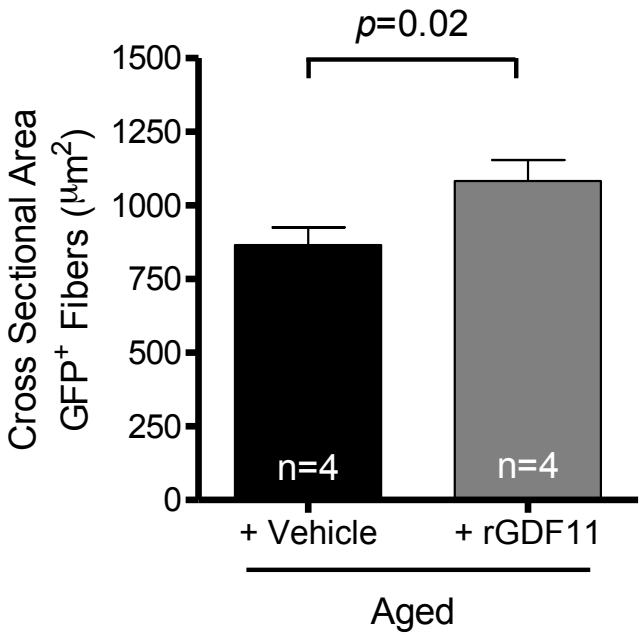

# Figure S11

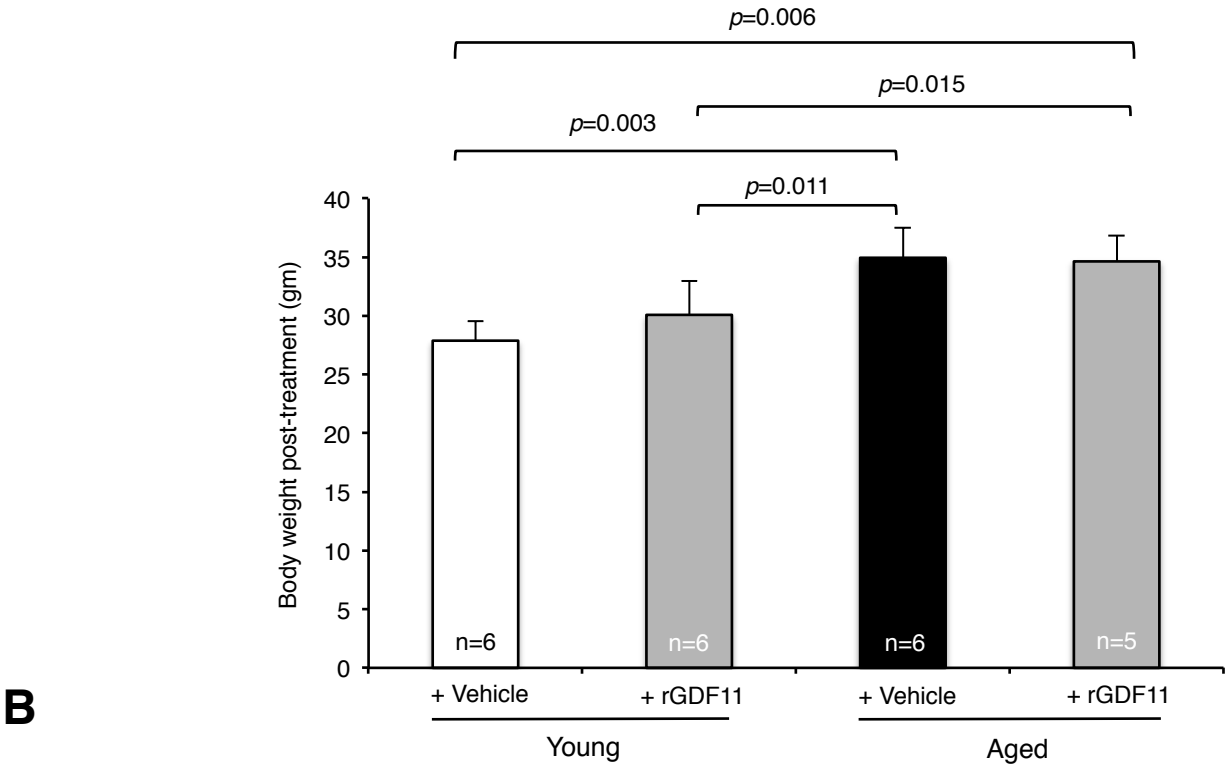
A
p=0.006
p=0.015
p=0.003
p=0.011
Body weight post-treatment (gm)
40
35
30
25
20
15
10
5
0
n=6
n=6
n=6
n=5
+ Vehicle
+ rGDF11
+ Vehicle
+ rGDF11
Young
Aged

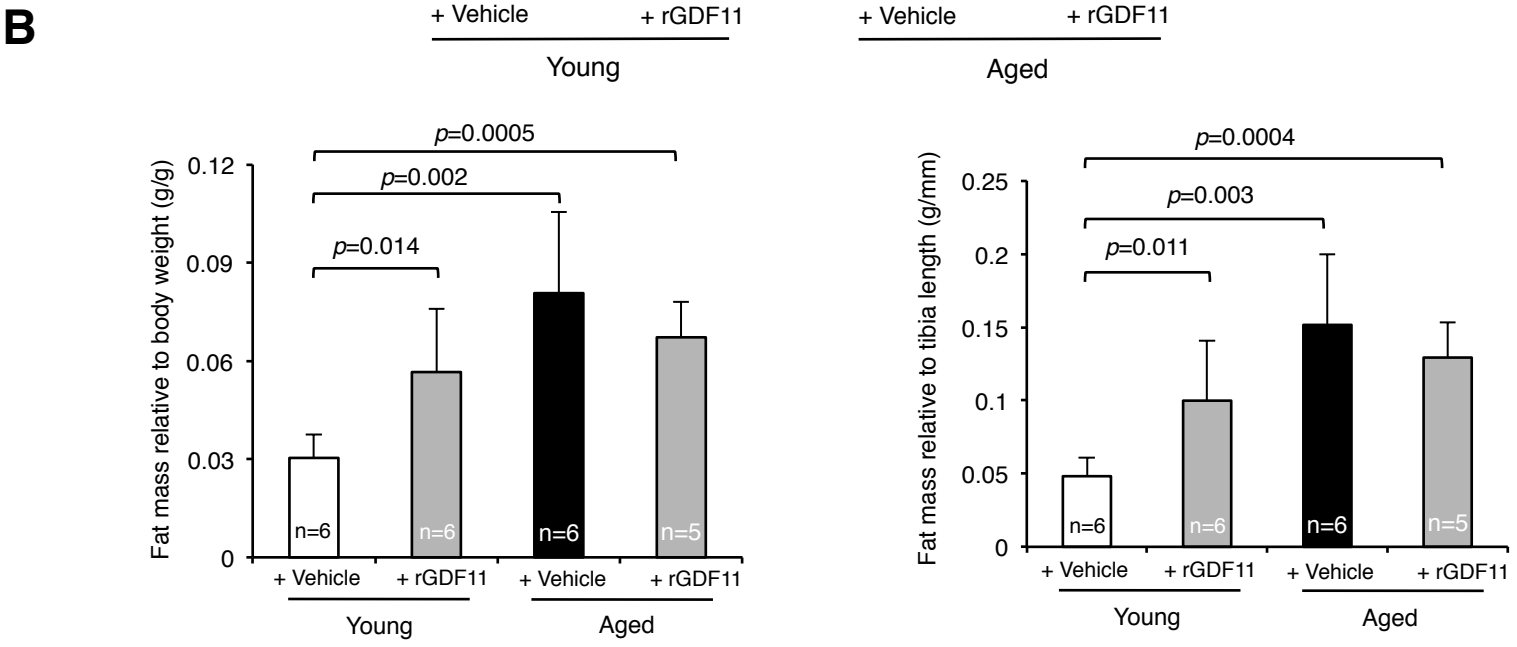
B
p=0.0005
p=0.002
p=0.014
Fat mass relative to body weight (g/g)
0.12
0.09
0.06
0.03
0
n=6
n=6
n=6
n=5
+ Vehicle
+ rGDF11
+ Vehicle
+ rGDF11
Young
Aged
p=0.0004
p=0.003
p=0.011
Fat mass relative to tibia length (g/mm)
0.25
0.2
0.15
0.1
0.05
0
n=6
n=6
n=6
n=5
+ Vehicle
+ rGDF11
+ Vehicle
+ rGDF11
Young
Aged

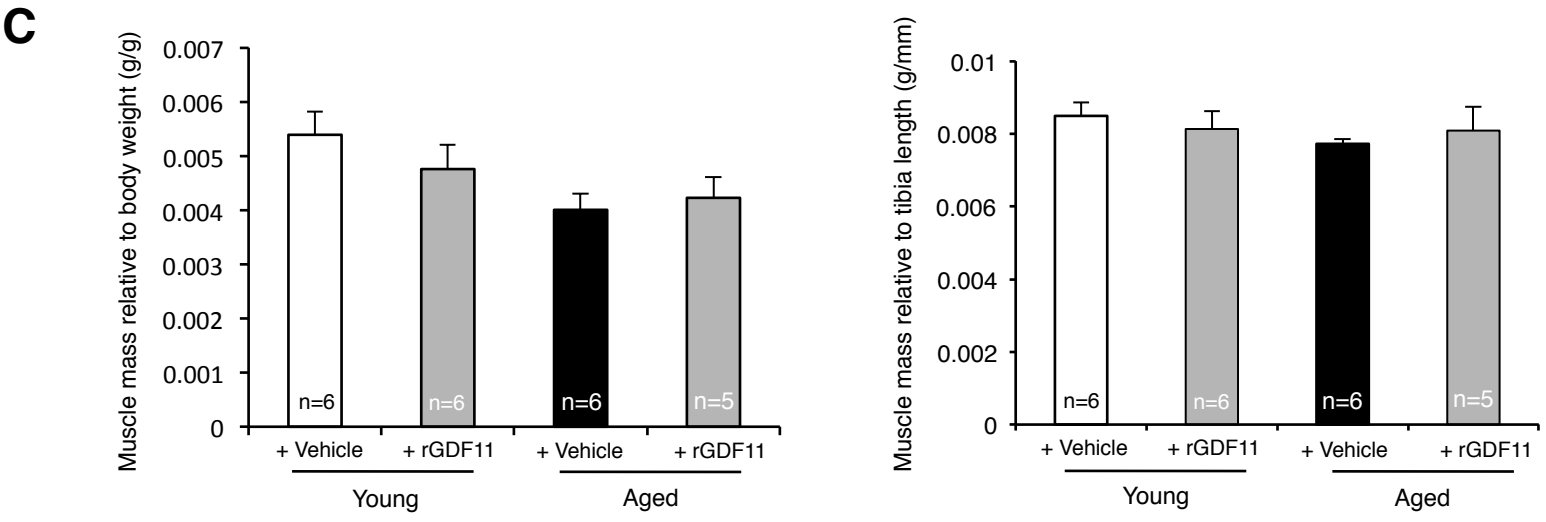
C
Muscle mass relative to body weight (g/g)
0.007
0.006
0.005
0.004
0.003
0.002
0.001
0
n=6
n=6
n=6
n=5
+ Vehicle
+ rGDF11
+ Vehicle
+ rGDF11
Young
Aged
Muscle mass relative to tibia length (g/mm)
0.01
0.008
0.006
0.004
0.002
0
n=6
n=6
n=6
n=5
+ Vehicle
+ rGDF11
+ Vehicle
+ rGDF11
Young
Aged

# Figure S12

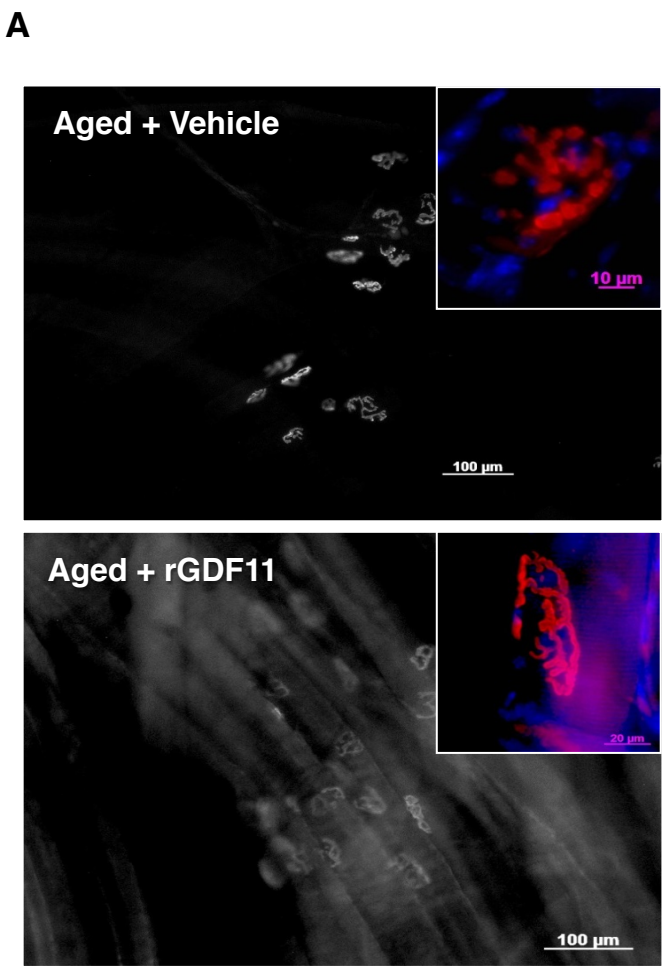
A
Aged + Vehicle
10 µm
100 µm
Aged + rGDF11
20 µm
100 µm

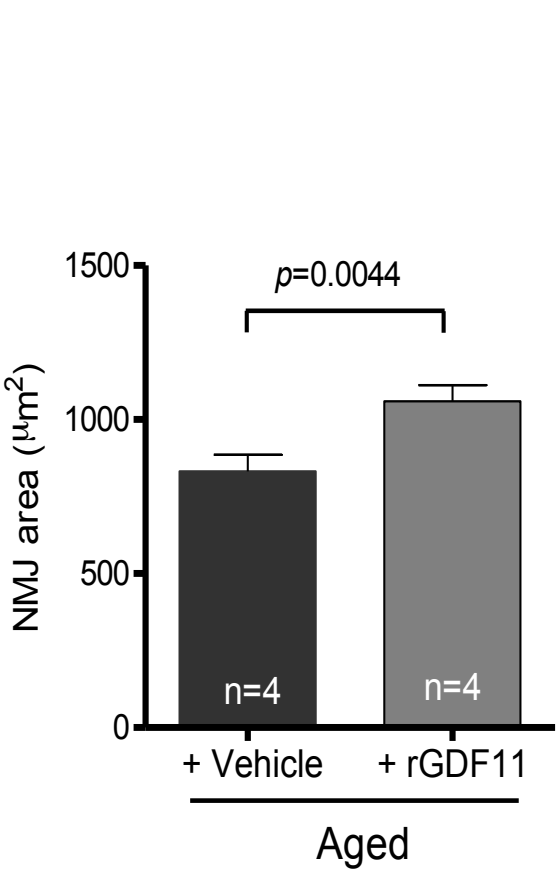
B
p=0.0044
1500
1000
500
0
NMJ area (µm2)
n=4
n=4
+ Vehicle
+ rGDF11
Aged

# Figure S13

**A**

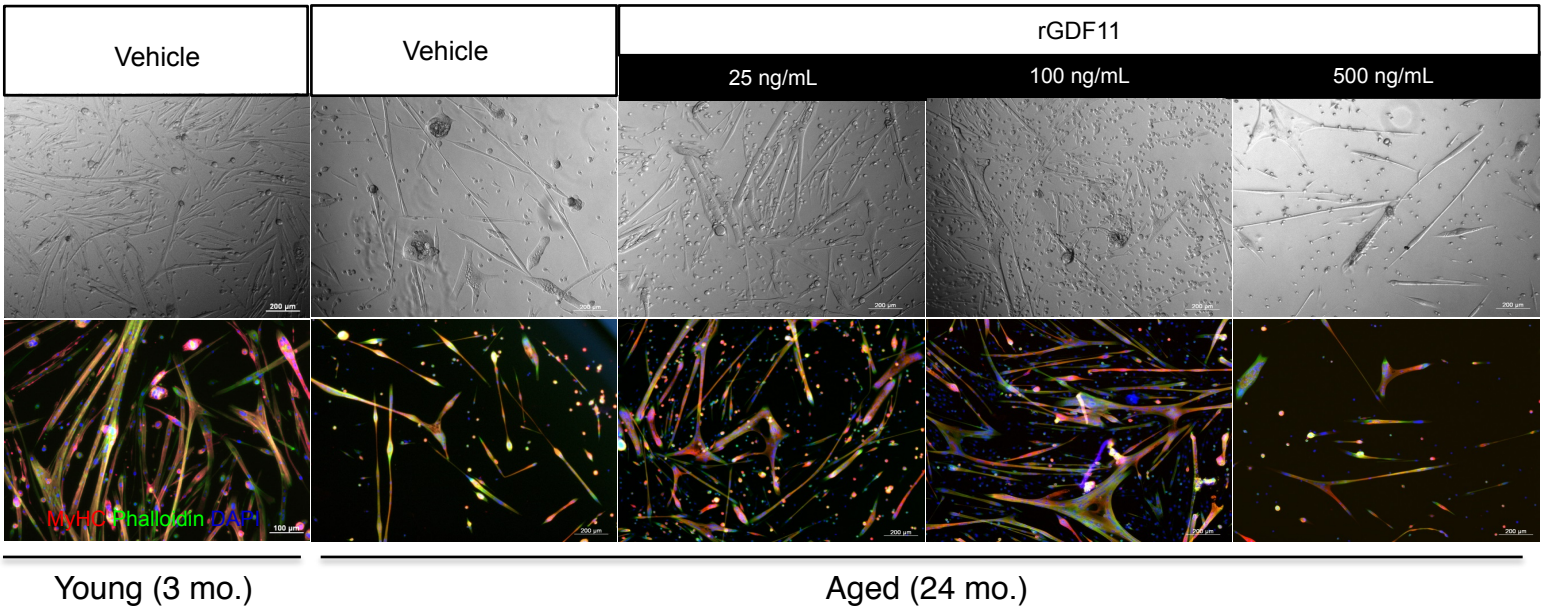


**B**

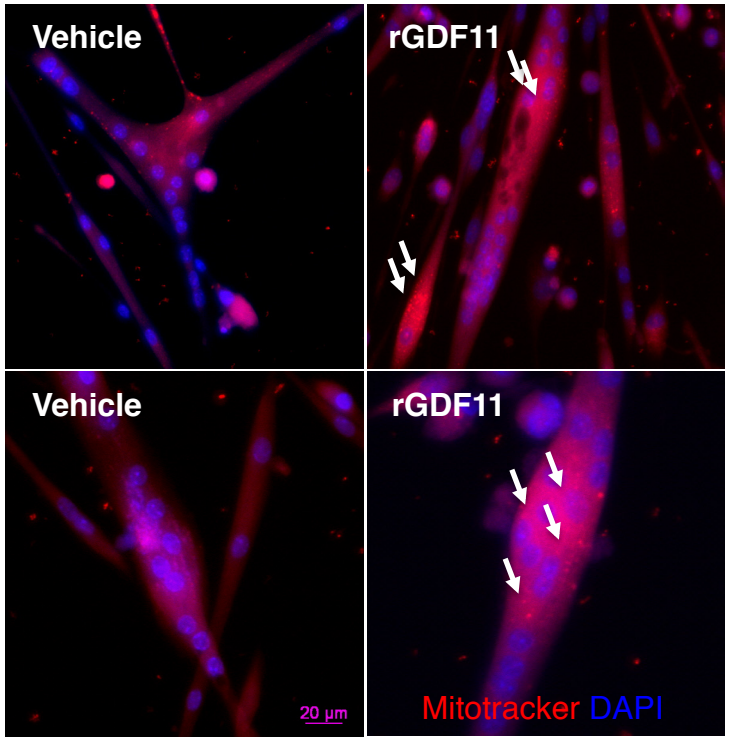


**C**

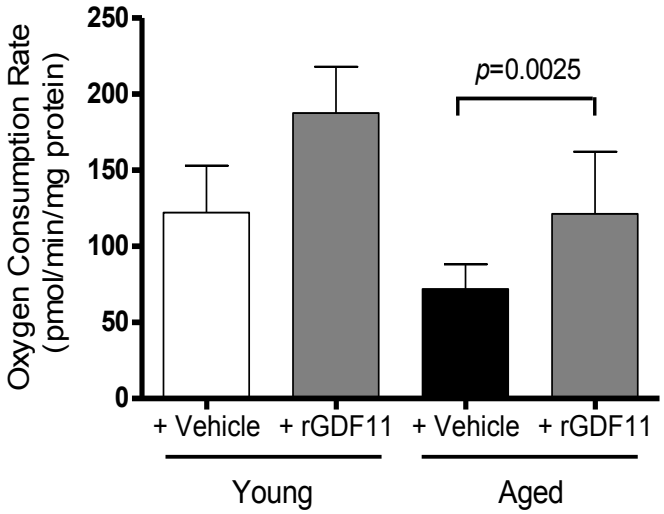

**Figure S14**

A

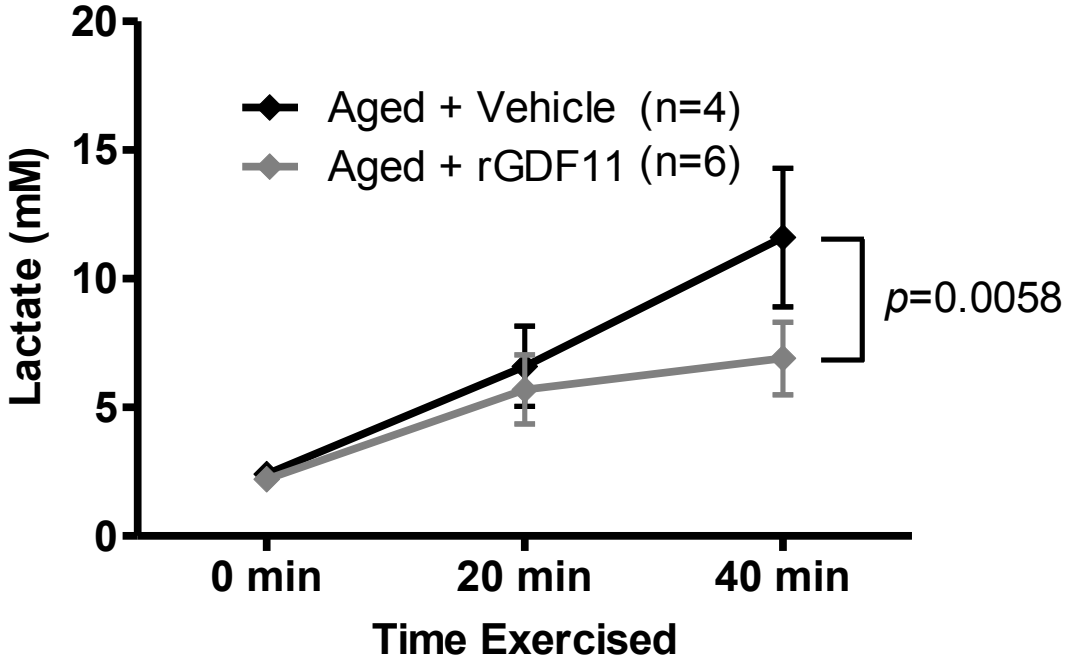


B

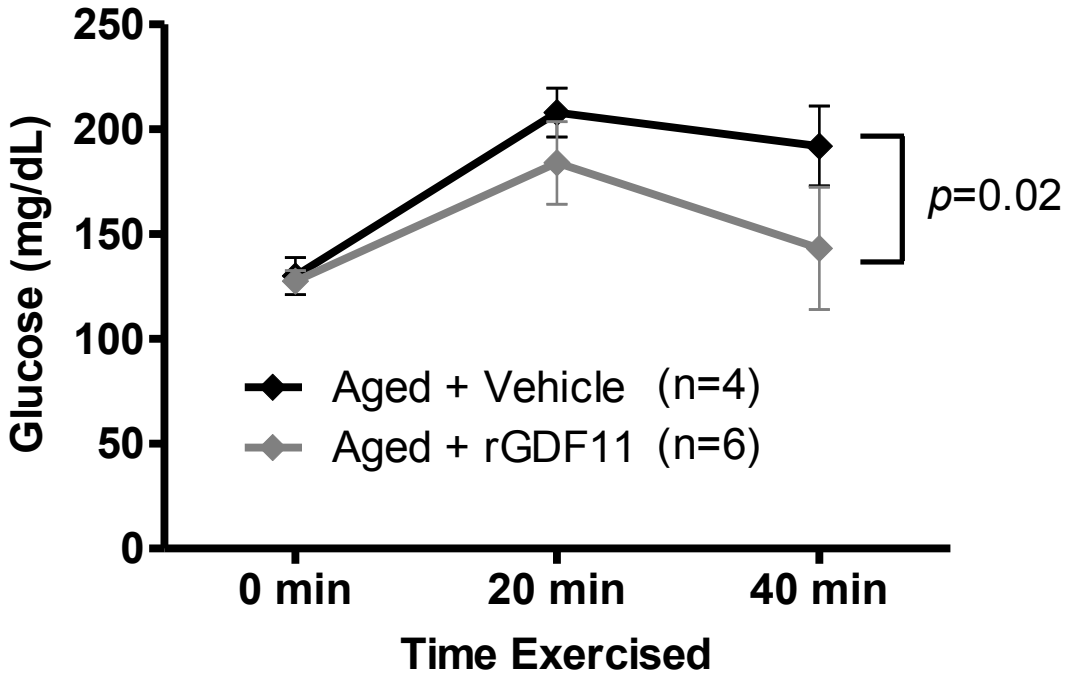

**Figure S15**

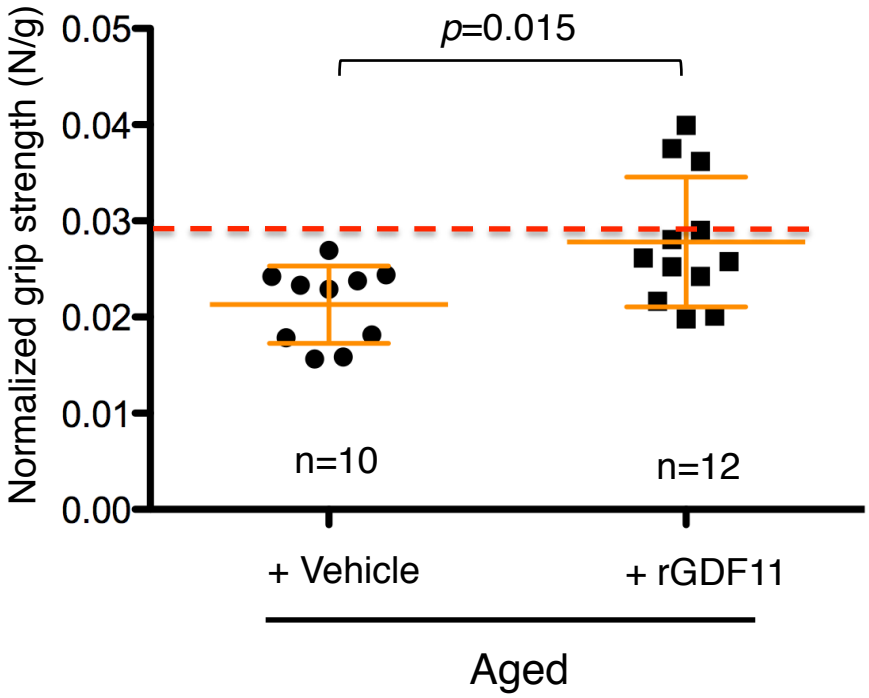
Normalized grip strength (N/g)
0.05
0.04
0.03
0.02
0.01
0.00
p=0.015
n=10
n=12
+ Vehicle
+ rGDF11
Aged

# Figure S16

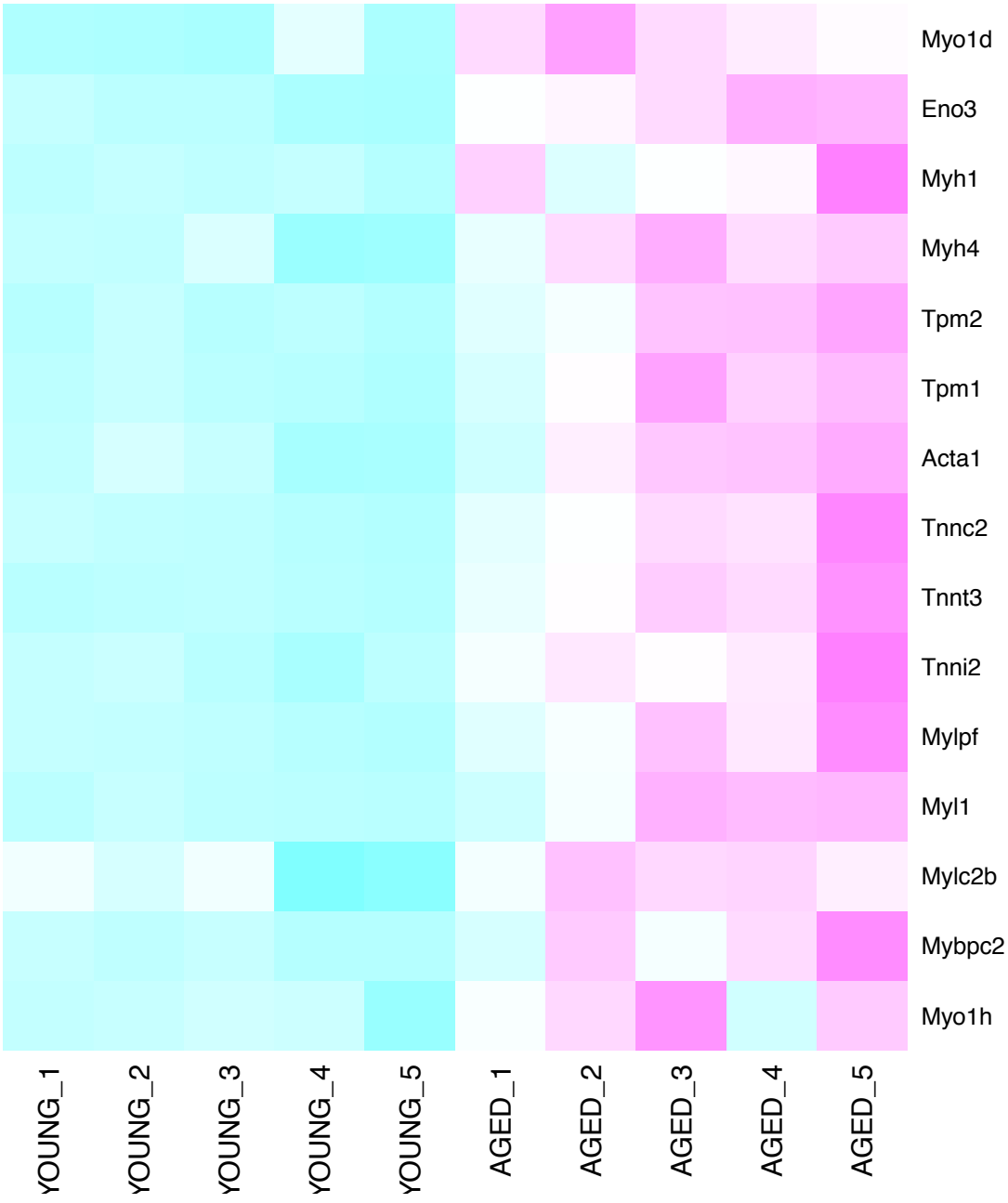
Myo1d
Eno3
Myh1
Myh4
Tpm2
Tpm1
Acta1
Tnnc2
Tnnt3
Tnni2
Mylpf
Myl1
Mylc2b
Mybpc2
Myo1h
YOUNG_1
YOUNG_2
YOUNG_3
YOUNG_4
YOUNG_5
AGED_1
AGED_2
AGED_3
AGED_4
AGED_5

Figure S17

A

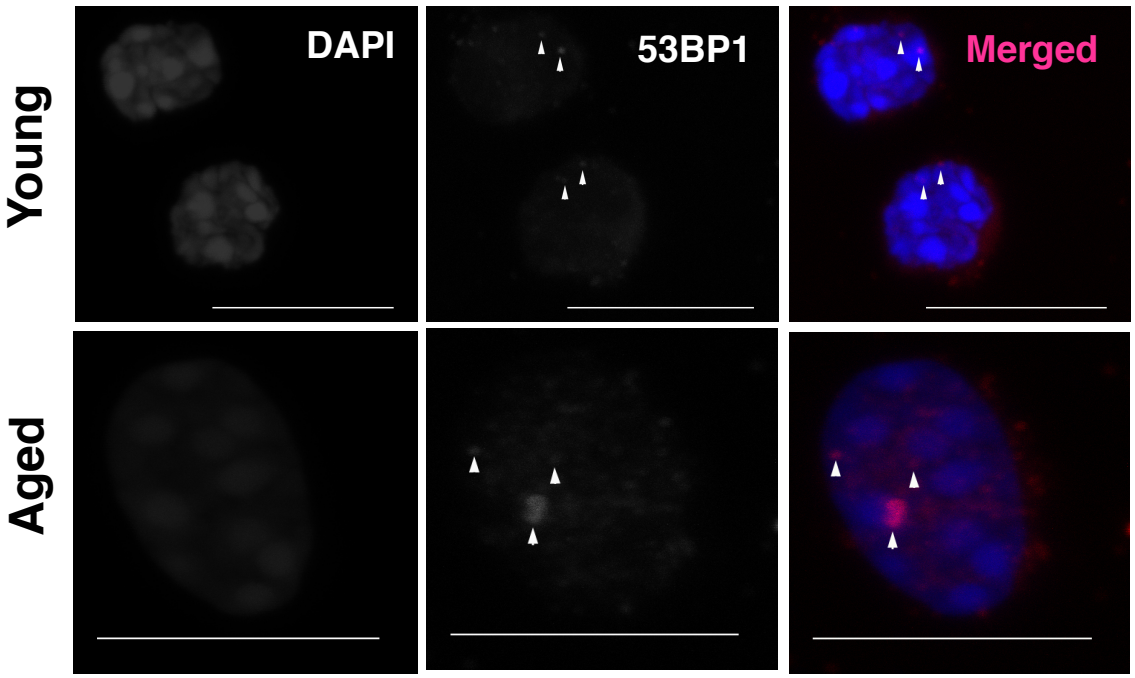


B

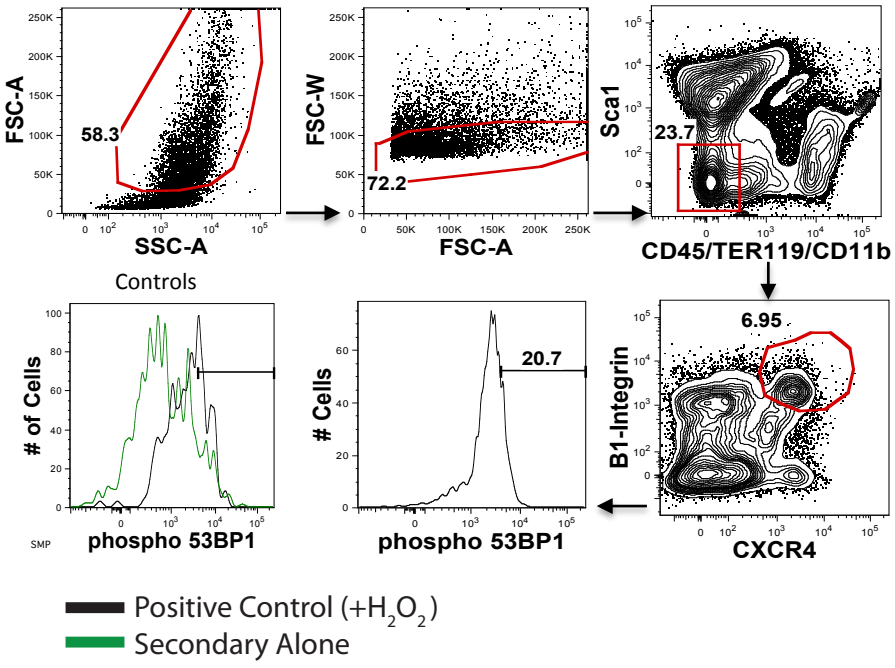


C

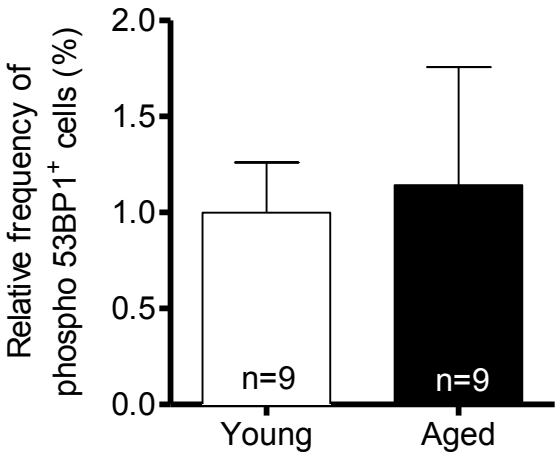

A

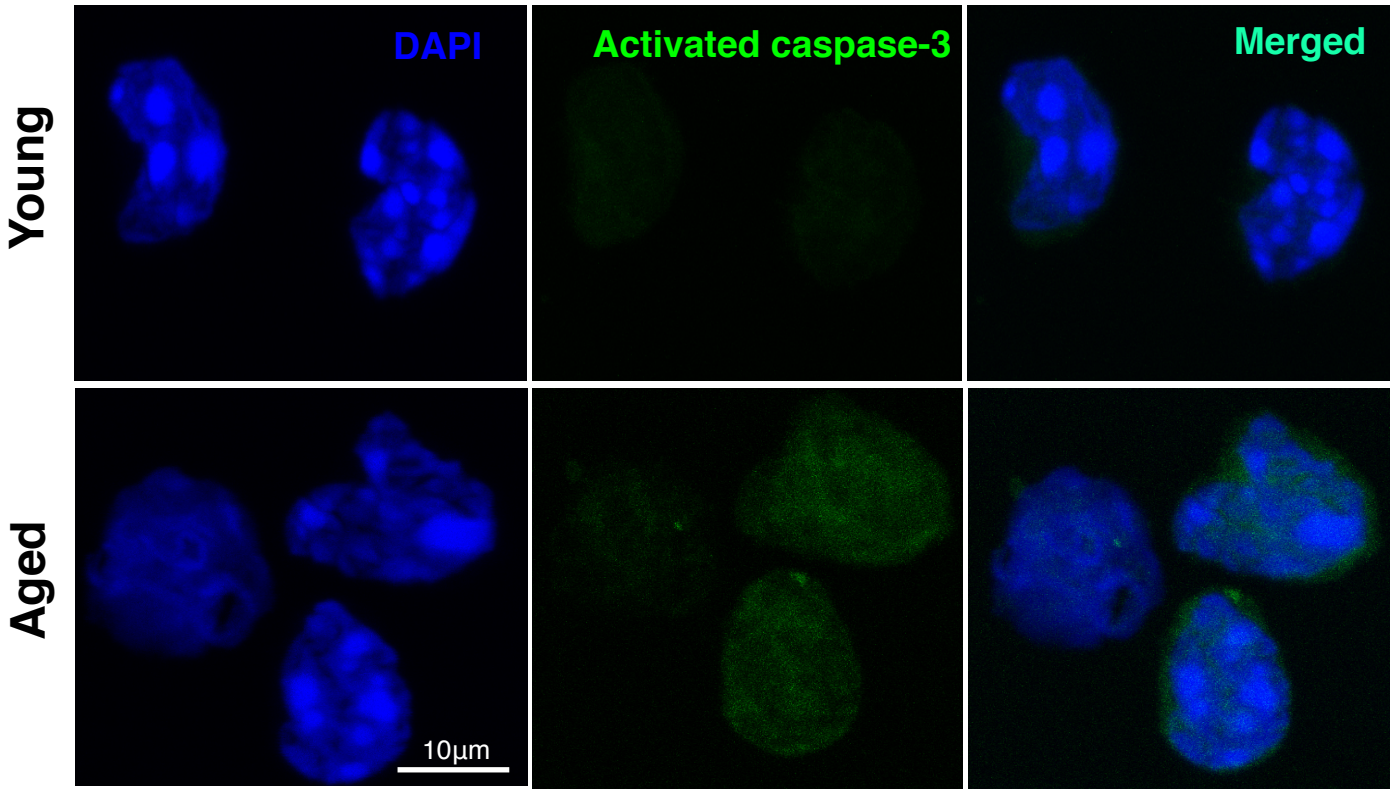
DAPI
Activated caspase-3
Merged
Young
Aged
10μm

B

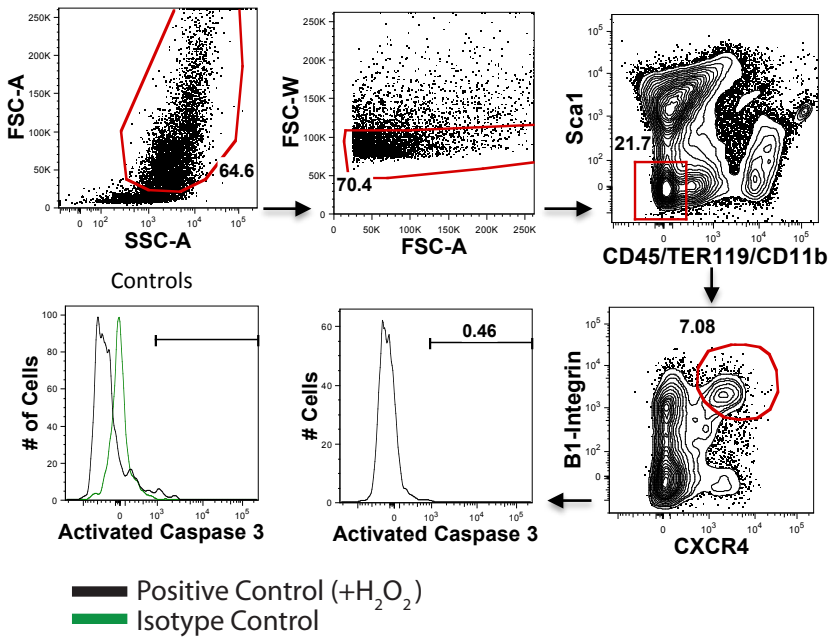
FSC-A
SSC-A
64.6
FSC-W
FSC-A
70.4
Sca1
CD45/TER119/CD11b
21.7
Controls
# of Cells
Activated Caspase 3
# Cells
Activated Caspase 3
0.46
B1-Integrin
CXCR4
7.08
Positive Control (+H2O2)
Isotype Control

C

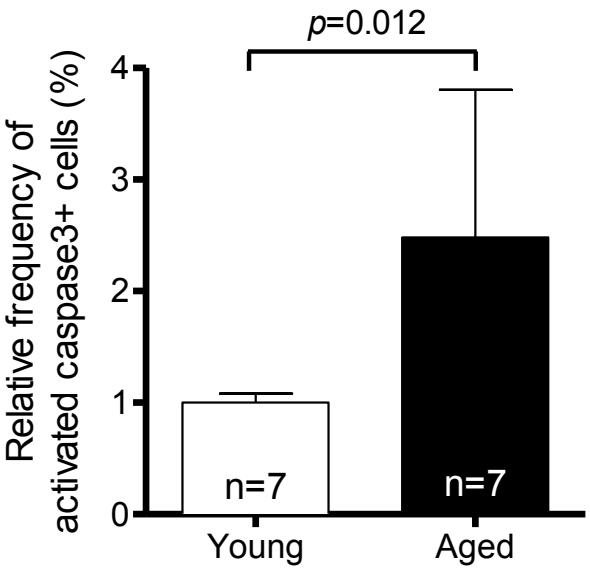
p=0.012
Relative frequency of activated caspase3+ cells (%)
n=7
n=7
Young
Aged

**Figure S19**

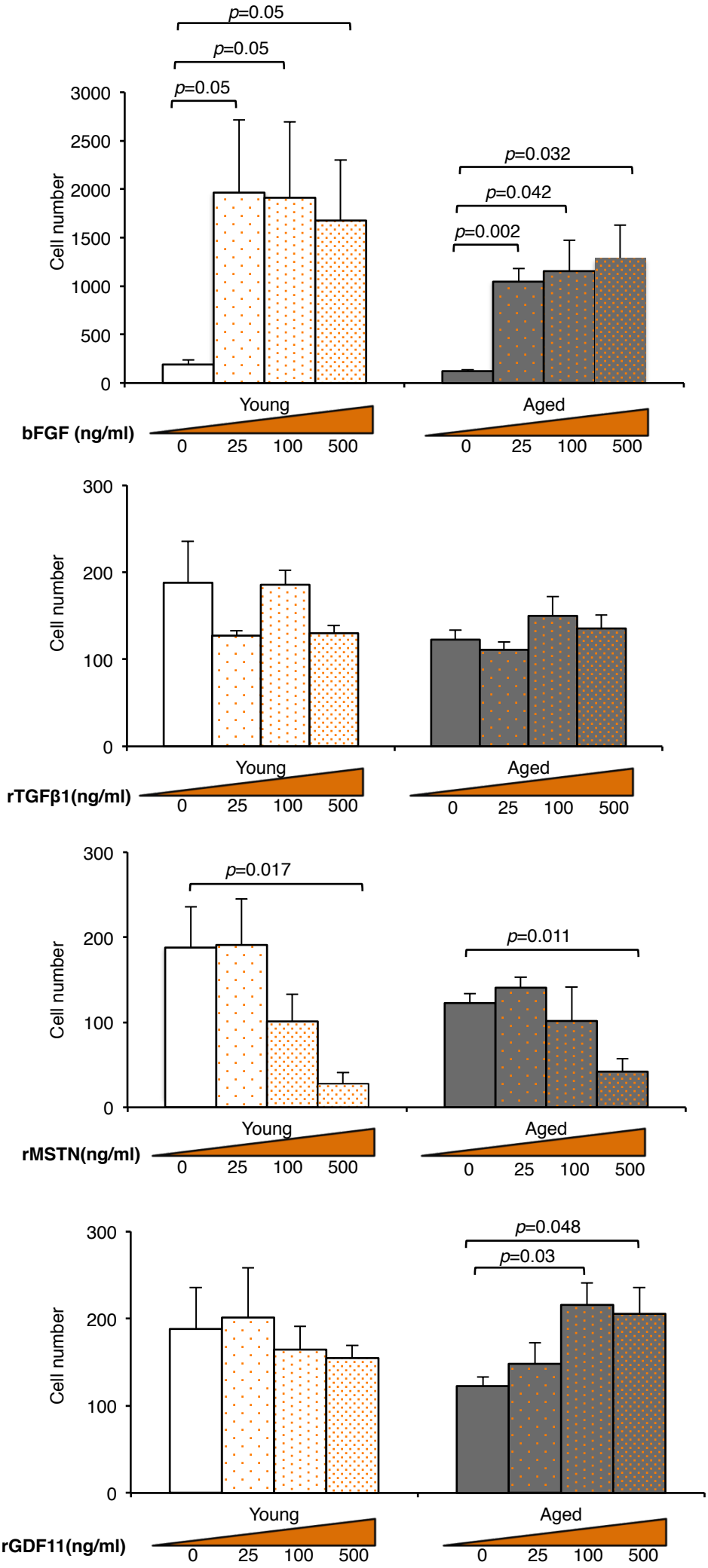
p=0.05
p=0.05
p=0.05
p=0.032
p=0.042
p=0.002
Cell number
3000
2500
2000
1500
1000
500
0
Young
Aged
bFGF (ng/ml)
0 25 100 500
0 25 100 500
300
200
100
0
rTGFβ1(ng/ml)
p=0.017
p=0.011
rMSTN(ng/ml)
p=0.048
p=0.03
rGDF11(ng/ml)

**Supplementary Figure Legends:**

**Fig. S1. Myogenic purity of freshly isolated satellite cells from young and aged mice.** **(A).** Representative immunofluorescence images of $Pax7^+$ (red) nuclei (blue) of FACS-purified $CD45^-Sca\text{-}1^-CD11b^-Ter119^-CXCR4^+\beta1\text{-}Integrin^+$ satellite cell populations isolated from young (top, 3 mo. of age) and aged (bottom, 27 mo. of age) mice. Merged images are shown at right. Consistent with prior reports (*4, 5*), the frequency of $Pax7^+$ cells among double-sorted $CD45^-Sca\text{-}1^-Mac1^-\ Ter119^-\ CXCR4^+\ \beta1\text{-}Integrin^+$ satellite cells was 98-100% for both young and aged mice. (**B**). Culture and differentiation of FACS-isolated $CD45^-Sca\text{-}1^-CD11b^-\ Ter119^-CXCR4^+\beta1\text{-}Integrin^+$ satellite cells confirms their myogenic commitment. Sorted satellite cells were seeded in myogenic growth medium (GM, containing F10, 20% horse serum, 1% Glutamax and 1% pen/strep) and grown for 5 days before re-plating into myogenic differentiation medium (DM, composed of DMEM, 1% GlutaMax, 1% pen-strep, and 2% FBS). After 3 days in differentiation medium, cells were fixed and immunostained for myosin heavy chain (MyHC, red) and nuclei stained for DAPI (blue). Consistent with prior publications (*3-5*), all sorted cells from young and aged mice maintained myogenic morphology and differentiated to form $MyHC^+$ myoblasts and myotubes. No adipocytes or fibroblasts were observed in any cultures of satellite cells from young or aged mice in any of the experiments reported here.

**Fig. S2. Reduced myogenic function and increased DNA damage in aged satellite cell nuclei**. The myogenic capacity of FACS-isolated satellite cells (Fig. S1 and (*4, 5*)) was assayed on a *per cell* basis using clonal myogenesis assays, in which double-sorted

satellite cells were seeded at one cell per well into individual wells of a 96-well plate and subsequently cultured in myogenic growth medium (*4, 5, 9*). Clone-sorted satellite cells form detectable colonies in this assay within 5 days of culture, and all colonies exhibit myogenic lineage commitment (see Fig S1 and (*4*)). Thus, comparison of the number of colonies formed by satellite cells sorted from different experimental mice (e.g., young and aged) reflects differences in the abilities of cells from these animals to survive and proliferate in response to myogenic stimuli. (**A**). Myogenic colony formation by clone-sorted satellite cells from young or aged mice. Data are presented as the percent of wells seeded with a single cell that yielded a detectable cell colony on day 5 of culture; all colonies detected from either young or aged donors were myogenic, and no fibroblasts or adipocytes were observed in any wells. Aged satellite cells formed up to 4-fold fewer colonies than young cells, indicating a diminished pool of myogenically active cells in aged mice. (**B**). Quantification (left) and representative images (right) of alkaline single cell gel electrophoresis assays performed with freshly sorted satellite cells harvested from young (2 mo. of age) or aged (24 mo. of age) mice. (**C**). Quantification (left) and representative images (right) of neutral single cell gel electrophoresis assays performed with satellite cells harvested from young (2 mo. of age) or aged (24 mo. of age) mice. DNA damage was quantified using a visual scoring metric (*25*) (key on top) and represented by color-coding: no damage (green), moderate damage (orange), maximal damage (red). Satellite cells from aged muscle showed increased DNA damage when assayed under alkaline (B) or neutral (C) conditions. (**D, E**). Representative immunofluorescence images **(**D**)** and quantification (E) of freshly sorted satellite cells stained with DAPI (blue, left column) and anti-pH2AX (green, middle column). Merged

images are shown at right. Fluorescence images are from a single plane at 63x. Aged satellite cells exhibited an increased frequency of cells with >2 pH2AX foci. Data represents mean ± SD from 3 biological replicates and *p*-values (color-coded in B and C) for statistically significant differences are shown at top. These data indicate that, as in the hematopoietic system (*15*), age-associated functional defects in muscle stem cells are associated with compromised DNA integrity.

**Fig. S3. Increased immunoreactivity to pH2AX in Pax7$^+$ satellite cell nuclei localized on aged muscle fibers**. (**A**). Representative immunofluorescence images at 63x of pH2AX in Pax7$^+$ (red) nuclei (blue) on isolated myofibers harvested from 2 young and 2 aged mice, as indicated at left. (**B**). Quantification of % pH2AX$^+$ nuclei among young or aged satellite cells stained as in (A). Data are compiled from 3 independent experiments. Each black diamond represents data from a single fiber (n=30-40 fibers analyzed per group in each experiment). Orange lines represent mean ± SD; *p*-value calculated by Mann-Whitney U test. These data confirm studies using FACS-isolated satellite cells (Fig. S2D,E), and indicate increased detection of pH2AX foci in aged satellite cells.

**Fig. S4. Reduced engraftment of irradiated young GFP$^+$ satellite cells into *mdx* mice.** (**A**). Representative images of transverse cryosections of TA from *mdx* recipients that were transplanted with non-irradiated (0 rad) or irradiated (50 or 100 rad) GFP$^+$ satellite cells (from 8-week old male GFP-transgenic donors) by intramuscular injection. (**B**). Bar graph representing the maximum number of GFP$^+$ fibers per recipient, as analyzed by direct epifluorescence on serial transverse sections. Data are shown as mean ± SEM from

n=3 animals per group and *p*-values were calculated using Students *t*-test. (**C**). Quantification of alkaline single cell gel electrophoresis assays performed with $GFP^+$ satellite cells used for transplantation, showing increased DNA damage among irradiated cells. Data represents mean ± SD from 3 experimental replicates. Color coded visual scoring key (*25*) of DNA damage assays and *p*-values, indicating only statistically significant differences, are shown at top and right.

**Fig. S5. Parabiosis chimerism**. Parabiotic animals were joined for 4-5 weeks, and cross circulation was confirmed in a subset of animals by analysis of congenic leukocyte surface antigens. Representative plots are shown indicating cross-engraftment of partner-derived cells in isochronic and heterochronic parabionts, in which one young partner was marked by expression of CD45.1 (blue) and the other partner by expression of CD45.2 (light brown). CD45 is a pan-leukocyte marker that allows discrimination of the origin of circulating white blood cells in the chimeric circulation. The percentage of CD45.1 versus CD45.2 congenic blood markers in splenocytes of young (blue or light brown) or aged (dark brown) partners from young-isochronic, young-heterochronic and aged-isochronic or aged-heterochronic parabiotic pairs is indicated for each gate. We were unable to assess chimerism in aged-isochronic pairs due to the unavailability of 22 mo. old CD45.1 mice; however, our extensive experience with this model (*11, 13, 24*), including prior studies using GFP-marked mice (*24*) have demonstrated previously that cross-circulation is effectively established in these fully isogenic pairs. Heterochronic pairs were always compared to age-matched isochronic pairs (young-young or aged-aged) to exclude any impact of the parabiosis surgery itself.

**Fig. S6. BrdU incorporation in young or aged satellite cells.** Recent studies using histone-labeled mice indicate that an increased fraction of satellite cells in resting muscle enter cell cycle in aged, as compared to young, mice (*6*). These data raise the possibility that accumulation of DNA damage in aged satellite cells may result from an increased number of stalled or collapsed replication forks in the more proliferative aged satellite cell pool. To test whether repair of DNA damage in aged satellite cells exposed to a young circulation might occur due to a return of these cells to their usual quiescent state after exposure to young systemic signals, we labeled all cycling cells in isochronic or heterochronic parabionts by feeding animals BrdU for the duration of their parabiotic joining (4 weeks). (**A**). Representative immuno-fluorescent images of BrdU staining in satellite cell nuclei harvested from young or aged partners of heterochronically joined mice and young or aged partners of isochronically joined mice. In all cases, the frequency of $BrdU^+$ nuclei is extremely low, and no differences could be detected among the 4 groups of mice. (**B**). Frequency of $BrdU^+$ satellite cells analyzed by flow cytometry for cells harvested from uninjured or cardiotoxin-injured hind limb muscles of 5 aged and 5 young mice (not joined in parabiosis). Data are presented as mean ± SD, with *p*-value calculated by Mann-Whitney test and indicated only for significant differences. BrdU incorporation was not different in uninjured muscle, and was reduced in satellite cells harvested from aged muscle, as compared to young, after injury. These data indicate that changes in satellite cell proliferative history are unlikely to explain the alterations in genome integrity or satellite cell function we observed after heterochronic parabiosis, and

support the notion that aged satellite cells show impaired activation in response to regenerative cues (*11*).

**Fig. S7 . Age-dependent alterations in local and systemic levels of TGF-ß1, Myostatin and GDF11.** To begin to uncover the systemic signals that restore muscle stem cell function in aged mice exposed to a youthful circulation, we searched for age-variant blood-borne factors in young and aged mice, focusing particularly on TGF-β family members. (**A**). Levels of TGF-β1 in plasma (left panel, dilution 1:40) or crushed muscle extract (right panel, dilution 1:10) as assayed by ELISA in young and aged male mice. (**B**). Levels of MSTN in plasma (left panel, dilution 1:40) or crushed muscle extract (right panel, 1:3) as assayed by ELISA in young and aged male mice. All graphs represent mean ± SEM and *p*-values, indicating only statistically significant differences, were calculated using *t*-test. (**C**). Western analysis of GDF11 levels in plasma and muscles of vehicle- or rGDF11-treated mice after 28 days of daily injections. Equal amounts (100 μg) of plasma proteins were loaded in each lane, with recombinant GDF11 (rGDF11) loaded at left as a control. Data is shown for 3 (top) or 4 (bottom) individual animals in each experimental category. These data demonstrate that endogenous levels of GDF11 are reduced with age in the skeletal muscle, as they are in plasma (*13*), and that rGDF11injection for 28 days is sufficient to increase the levels of mature GDF11 (12.5kDa) in the plasma of young and old animals (top), and in the muscle of aged mice (bottom). It is interesting to note that plasma levels of GDF11 in aged mice administered rGDF11 at 0.1 mg/kg daily generally remained lower than those in young (2 month old)

mice, suggesting that complete replenishment of GDF11 to youthful levels may not be essential for some of its rejuvenating effects.

**Fig. S8. Frequency of niche components after GDF11 treatment.** Flow cytometric analysis of frequency of hematopoietic ($CD45^+CD11b^+Ter119^+$), fibrogenic-adipogenic and endothelial ($CD45^-CD11b^-Ter119^-Sca\text{-}1^+$) or differentiated myoblast and fibroblast ($CD45^-CD11b^-Ter119^-Sca\text{-}1^-ß1\text{-}Integrin^+CXCR4^-$) cells (*4*) from the skeletal muscle of young and aged mice treated with vehicle or rGDF11. Data represents mean ± SD, with *p*-value calculated by Student's *t*-test and indicated only for significant differences. Treatment with rGDF11 did not induce significant changes in the frequencies of these muscle niche components in either young or aged mice.

**Fig. S9. rGDF11 increases the cross sectional area of regenerating fibers in aged muscle, but does not affect the size of myofibers in uninjured muscle in young or aged mice.** (**A**). Bar graph representing average cross-sectional area in $\mu m^2$ of all regenerating fibers analyzed for Figures 2D and E. Number of animals used for analysis is shown within each bar. (**B**). Frequency distribution (left) of muscle fibers and the average cross-sectional area in $\mu m^2$ (right) of young contralateral control tibialis anterior (TA) muscle, which was not injured. (**C**). Frequency distribution (left) of muscle fibers and the average cross-sectional area in $\mu m^2$ (right) of aged contralateral control TA, which was not injured. Average cross-sectional area data represents mean ± SEM and *p*-values as shown were calculated using Students t-test. Frequency distribution was analyzed by Wilcoxon exact test, and showed no statistically significant differences for

young + vehicle *versus* young+rGDF11 or for aged + vehicle *versus* aged + rGDF11, for uninjured muscles. Thus, rGDF11 stimulates accelerated recovery of myofiber size in regenerating muscle after injury, but at the doses studied here, has no impact on myofiber size or muscle mass (see Fig. S11C) in uninjured tissue.

**Fig. S10**. **rGDF11 increases the cross sectional area of engrafted, regenerating fibers in aged muscle.** (**A**). Schematic diagram depicting experimental design. $GFP^+$ satellite cells were sorted from GFP transgenic mice and transplanted into aged recipients (n=4 per group) who were treated with rGDF11 or vehicle alone for 4 weeks prior and 2 weeks following transplantation. (**B**). Representative images of transverse cryosections of TA muscle harvested 2 weeks after transplantation with 30,000 double-sorted $GFP^+$ satellite cells isolated from young mice (4-6 weeks of age). Satellite cells were injected into the TA muscles of vehicle- (top) or rGDF11 (bottom)-treated aged mice, which were pre-injured by cardiotoxin injection 1 day prior to satellite cell transplantation, as in (*4, 5*). Muscles were analyzed for GFP expression by direct epifluorescence at 40x magnification. (**C**). Quantification of myofiber cross-sectional area for newly regenerated $GFP^+$ fibers (shown in B). Data represent mean ± SD and *p*-value was calculated by Student's *t*-test.

**Fig. S11. No detectable alterations in body-weight, fat-mass or muscle-mass after rGDF11 supplementation in young or aged animals.** (**A**). Bar graph representation of body weight in grams after 30 days of vehicle- or rGDF11-treatment in young or aged male mice. All mice were housed and treated in the same facility. (**B**). Bar graph

representation of fat-mass normalized to body weight (left panel) or tibia length (right panel) as indicated. Fat-mass represents sum of excised white fat pads at inguinal, gonadal and axillary locations of both sides of each animal. (**C**). Bar graph representation of muscle-mass normalized to body weight (left panel) or tibia length (right panel) as indicated. Muscle mass represents a sum of TA and EDL muscle-mass of both hindlimbs of each animal. Number of animals used for analysis is shown within each bar as "n=". Data represents mean ± SD. *p*-values, calculated by Students *t*-test, are shown only for statistically significant differences.

**Fig. S12. rGDF11 increases the size of NMJs in aged muscle.** (**A**). Representative immunofluorescence images of neuromuscular junctions (NMJ) on TA muscles of vehicle- or rGDF11-treated aged mice. Higher magnification (40X objective lens) of one NMJ is shown in the top right insets. Postsynaptic acetylcholine receptors are labeled with AlexaFluor 555-conjugated α-Bungarotoxin (red) and myonuclei are stained with DAPI (blue). (**B**). Quantification of surface area of postsynaptic acetylcholine receptors. Total number of animals used for analysis is shown within each bar as "n=". Data are presented as mean ± SEM and *p*-values were calculated by Student's *t*-test.

**Fig. S13. rGDF11 promotes myogenic differentiation and mitochondrial function *in vitro*.**

(**A**). Representative brightfield (top) or immunofluorescence (bottom) images of satellite cells harvested from young (3 mo.) or aged mice, proliferated with vehicle (control) or rGDF11 at the concentration indicated for 5 days in growth media followed by

differentiation media for 5 days (young) or 7 days (aged). Cells were stained after culture to identify nuclei (DAPI, blue), cellular actin (Phalloidin, green), and myosin heavy chain (MyHC, red). Cultures of aged satellite cells exposed to rGDF11 at 25 or 100ng/mL showed enhanced myogenic differentiation. (**B**). Representative immunofluorescence images of Mitotracker$^{TM}$ stained myotubes, differentiated in the presence of vehicle alone or 100ng/ml rGDF11. Mitotracker is a mitochondrial membrane potential dependent dye and arrows indicate puncta of mitochondria in differentiated myotubes. (**C**). Bar graph of basal oxygen consumption rate (OCR) in Seahorse metabolic flux assays of young or aged satellite cells differentiated for 7 days in the presence of vehicle alone or of 100ng/ml rGDF11. Cells exposed to rGDF11 show increased Mitotracker staining and increased OCR, indicative of enhanced mitochondrial content and bioenergetics. Data represents average of 5 technical replicates ± SD and only significant *p*-values are shown, calculated using Student's *t*-test.

**Fig. S14. Increased lactate clearance and decreased glucose levels during exercise in aged mice treated with rGDF11.** (**A, B**). Quantification of blood lactate (A) or glucose (B) levels of vehicle- (black line) or rGDF11- (grey line) treated aged mice, sampled at the indicated times during treadmill exercise, as in Fig. 3D. Data are presented as mean ± SD. Total number of animals used for analysis is shown within parenthesis as "n=" and *p*-values were calculated by Student's *t*-test.

**Fig. S15**. **Improved grip strength of aged mice upon rGDF11 supplementation**. Scatter plot of forelimb grip-strength of vehicle- or rGDF11-treated aged mice plotted as

maximum force normalized to body weight (Newton/gram (N/g)) exerted in triplicate trials. Red line represents the normalized maximum grip-strength of 33-39 week-old young male mice. Data are presented for individual mice (black symbols) overlaid with mean ± SD (orange lines). *p*-value calculated by Mann-Whitney analysis, and "n=" indicates number of mice used for this analysis. Aged mice treated with rGDF11 show increased normalized grip strength.

**Fig. S16. Upregulation of myogenic gene expression in freshly isolated aged satellite cells**.

Heat map representation of differentially expressed myogenic genes. Data are represented in a gradient of blue to pink (blue indicating low and pink indicating high level of expression), for FACS-isolated young (2 mo. of age, left columns) or aged (22-24 mo. of age, right columns) satellite cells (n=5 independent samples per group). Individual gene symbols are indicated on the right in young and aged satellite cells. Aged satellite cells generally show an increase in myogenic gene expression.

**Fig. S17. Similar detection of 53BP1 and phosphorylated-53BP1 in young and aged satellite cells.** (**A**). Representative confocal immunofluorescence images (sums of z-stacks) of 53BP1foci (marked with white arrowheads) of young and aged satellite cells as indicated. Scale bar = 10μm

(**B**). Representative flow plots from analysis of a young mouse illustrating gating strategy for flow cytometric analysis of phospho-53BP1 in $CD45^{-}Sca\text{-}1^{-}CD11b^{-}Ter119^{-}$ $CXCR4^{+}\beta1\text{-}Integrin^{+}$ satellite cells. (**C**). Quantification of flow cytometric analysis

presented as frequency of phosphorylated-53BP1$^{+}$ satellite cells among total satellite cells from young or aged animals (n=9 animals per group). Data were normalized to the average frequency of phosphorylated-53BP1$^{+}$ satellite cells for young mice and are presented as relative mean ± SD. Differences were not statistically significant, calculated using Mann-Whitney analysis.

**Fig. S18. Increased immunoreactivity to activated caspase-3 in aged satellite cell nuclei.**

(**A**). Representative confocal (sums of z-stacks) immuno-fluorescent images of activated caspase-3 staining in satellite cells harvested from young or aged mice. Scale bar = 10μm (**B**). Representative flow plots from a young mouse illustrating gating strategy for flow cytometric analysis of activated caspase-3 in CD45$^{-}$Sca-1$^{-}$CD11b$^{-}$Ter119$^{-}$CXCR4$^{+}$β1-Integrin$^{+}$ satellite cells. (**C**). Quantification of flow cytometric analysis presented as frequency of activated caspase3$^{+}$ satellite cells among total satellite cells from young or aged animals (n=7 animals per group). Data were normalized to the average frequency of activated caspase3$^{+}$ satellite cells for young mice and are presented as relative mean ± SD). *p*-value was calculated using Mann-Whitney analysis.

**Fig. S19. Effects of bFGF, rTGF-β1, rMSTN and rGDF11 on satellite cell proliferation *in vitro*.** Quantification of cell number after *in vitro* culture of satellite cells for 5 days in presence of indicated concentrations of bFGF, or recombinant TGF-β1, recombinant MSTN, or rGDF11 (as indicated). 200 double sorted satellite cells per well (>98% purity) from young (8-12 weeks) or aged (24 mo.) mice were seeded initially and

cultured in growth medium containing 20% knock-out serum replacement lacking members of the TGF-β superfamily of growth factors. Data presented as mean ± SD. *p*-values, calculated by Student's *t*-test, are shown only for statistically significant differences.